



2

# Shallow-Water Transmission Measurements Taken on the New Jersey Continental Shelf

A Presentation to the 121st Meeting of the  
Acoustical Society of America, 2 May 1991,  
Baltimore, Maryland

William Carey  
Lynne Malocco Dillman  
Surface Anti-submarine Warfare System

James Doult  
Woods Hole Oceanographic Institution

DTIC  
ELECTE  
MAY 27 1992  
S D



Naval Undersea Warfare Center Detachment  
New London, Connecticut

92-13867



Approved for public release; distribution is unlimited.

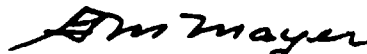
92 5 26 082

## Preface

This research was conducted under NUWC Project No. A64400, "Hudson Canyon Project," Principal Investigator Dr. William Carey (Code 302). The data for this study were gathered as part of the NUWC/ONR experiment conducted on the New Jersey continental shelf. Funding for this effort was obtained from Dr. M. Orr (Code 11250A) of the Office of Naval Research and from Dr. K. Lima, Independent Research Program (Code 10).

The Technical Reviewer for this report was Peter Herstein (Code 33A).

Reviewed and Approved: 13 April 1992



Gerald Mayer  
Head, Environmental & Tactical Support Systems Department

# REPORT DOCUMENTATION PAGE

Form Approved  
OMB No. 0704-0188

Public reporting burden for this collection of information is estimated to average 1 hour per response, including the time for reviewing instructions, searching existing data sources, gathering and maintaining the data needed, and completing and reviewing the collection of information. Send comments regarding this burden estimate or any other aspect of this collection of information, including suggestions for reducing this burden, to Washington Headquarters Service, Directorate for Information Operations and Reports, 1215 Jefferson Davis Highway, Suite 1204, Arlington, VA 22202-4302, and to the Office of Management and Budget, Paperwork Reduction Project (0704-0188), Washington, DC 20503.

1. AGENCY USE ONLY (Leave blank)		2. REPORT DATE 13 April 1992		3. REPORT TYPE AND DATES COVERED	
4. TITLE AND SUBTITLE Shallow Water Transmission Measurements Taken on the New Jersey Continental Shelf				5. FUNDING NUMBERS PR A60460	
6. AUTHOR(S) William Carey, James Douth, Lynne Maiocco Dillman					
7. PERFORMING ORGANIZATION NAME(S) AND ADDRESS(ES) Naval Undersea Warfare Center Detachment New London, CT 06320				8. PERFORMING ORGANIZATION REPORT NUMBER TD 10,025	
9. SPONSORING / MONITORING AGENCY NAME(S) AND ADDRESS(ES) Office of Naval Research 1125 OA Office of the Chief of Naval Research Arlington, VA 22217-5000				10. SPONSORING / MONITORING AGENCY REPORT NUMBER	
11. SUPPLEMENTARY NOTES					
12a. DISTRIBUTION / AVAILABILITY STATEMENT Approved for public release; distribution is unlimited.				12b. DISTRIBUTION CODE	
13. ABSTRACT (Maximum 200 words)  Calibrated acoustic measurements were made under calm sea state conditions on the New Jersey shelf near Amcor 6010, a surveyed area with known geophysical properties. The experiment was conducted in 73 m water with supporting measurements of salinity, temperature, and sound speed. These measurements were obtained with a vertical array of 24 equally spaced hydrophones at 2.5 m; one of which was on the bottom. A source towed at either 1/2- or 3/4- water depth transmitted one of two sets of four tones spaced between 50 and 600 Hz for each run to ranges of 4 and 26 km. The data were processed with Hankel transform and Doppler processing techniques to yield horizontal wave-number spectrum at several depths. Results were obtained along both a constant and gradually varying depth radial. Similar modal interference patterns were observed at the lower frequencies. The constant radial results were compared to calculations using several shallow propagation models employing both geoacoustic profiles derived from geophysical parameters and Yamamoto's (1990) shear wave inversion. Predicted and measured levels generally agreed; however, differences in computed and measured modal interference patterns were observed.					
14. SUBJECT TERMS Sound Propagation    Horizontal wavenumber spectrum shallow water    vertical array    Hankel transform Doppler    modes    mode shapes    geoacoustic				15. NUMBER OF PAGES	
				16. PRICE CODE	
17. SECURITY CLASSIFICATION OF REPORT UNCLASSIFIED	18. SECURITY CLASSIFICATION OF THIS PAGE UNCLASSIFIED	19. SECURITY CLASSIFICATION OF ABSTRACT UNCLASSIFIED	20. LIMITATION OF ABSTRACT SAR		

**SHALLOW-WATER TRANSMISSION MEASUREMENTS  
TAKEN ON THE NEW JERSEY CONTINENTAL SHELF**

**WILLIAM CAREY  
JAMES DOUTT  
LYNNE MAIOCCO DILLMAN**

**2 MAY 1991  
121st MEETING ASA**

**VIEWGRAPH 1**

## VIEWGRAPH 2: THE HCE PARTICIPANTS

# THE HUDSON CANYON EXPERIMENT

A PROJECT OF THIS SIZE REQUIRES A LARGE SUPPORT TEAM OF DEDICATED INDIVIDUALS.

WILLIAM M. CAREY	-	NUSC	PRINCIPAL INVEST.
E. HUG	-	NUSC	NAVIGATION
S. RAJAN	-	WHOI	OCEANOGRAPHICS
J. DOUTT	-	WHOI	DATA ANALYSIS
E. PARSSINEN	-	KILDARE	SOUND SOURCE
J. FITZGERALD	-	KILDARE	SOUND SOURCE
J. CARNELL	-	C&M	SEA CAL SYS.
R. EVANS	-	SAIC	ACOUSTIC MODELING
B. BORDEAUE	-	MAR	CAPTAIN (RV RANGER)
R. MILLER	-	NUSC	OPERATIONS

<b>TECHNICAL SUPPORT</b>			DATA ACQ. AND ANALYSIS
L. MAIOCCO	-	NUSC	COMPUTER RUNS
H. BUI	-	NUSC	PLANNING
M. BAIDEY	-	UNIV. MIAMI	SEA CAL SYS.
J. MINGRONE	-	C&M	PROG. AND ANALYSIS
W. KANABIS	-	NUSC	PROG. AND ANALYSIS
J. BISHOP	-	NUSC	COMPUTER RUNS
J. PRENTICE	-	NUSC	

<b>SPONSORS</b>		11250A
M. ORR	-	CODE 10/IR
K. LIMA	-	

## Viewgraph 2 The HCE Participants

An ocean-acoustics experiment requires the talents of many dedicated professionals as well as a dedicated sponsor. The sponsors for this experiment were K. Lima (NUSC/IR) and M. Orr (ONR 1125 OA). The research team that conducted this experiment and each member's area of responsibility is shown on this viewgraph. Our objective was to obtain calibrated sound transmission data near the AMCOR 6010 borehole, a recently surveyed area with known geophysical properties. We were asked to conduct the experiment in May of 1988 and, with a lot of hard work and luck, conducted the experiment in September 1988. In acknowledging individuals who made this experiment possible, I must mention Helen Darmera, Office of the Comptroller, D.O.N. During the spring of 1988 the Secretary of Defense froze all Navy R&D contract obligations. We happened to be one of the few exceptions, perhaps the only exception, granted funds for basic research during this time. Helen Darmera was a tremendous help in getting the comptroller's attention and the granting of a waiver. (See letter below.)



DEPARTMENT OF THE NAVY  
OFFICE OF THE COMPTROLLER  
WASHINGTON, D.C. 20350-1100

IN REPLY REFER TO  
07 JUN 1988

From: Comptroller of the Navy  
To: Chief of Naval Research  
Subj: OBLIGATION WAIVER FOR HUDSON CANYON  
Ref: (a) NUSC 2719202 MAY 88  
(b) ALNAV 066/88

1. I have reviewed the request forwarded by reference (a) to grant a waiver from the prohibition on obligation promulgated by reference (b). The obligation of \$79 thousand is required for fabrication of cable and refurbishment of hydrophones for a measurement system in support of a 20 August experiment. Since the 20 August sea test required that three ship schedules be coordinated to support several interrelated ONR experiments, delay in providing the measurement system would mean cancellation of the shallow water acoustic measurement portion of the project required for proof of concept. Validation of the concept would require repetition of the ocean floor measurement experiments being carried out simultaneously at an approximate cost of \$750 thousand. As it is not cost-effective to require repetition of these tests to save \$79 thousand, you are granted a waiver for this action.

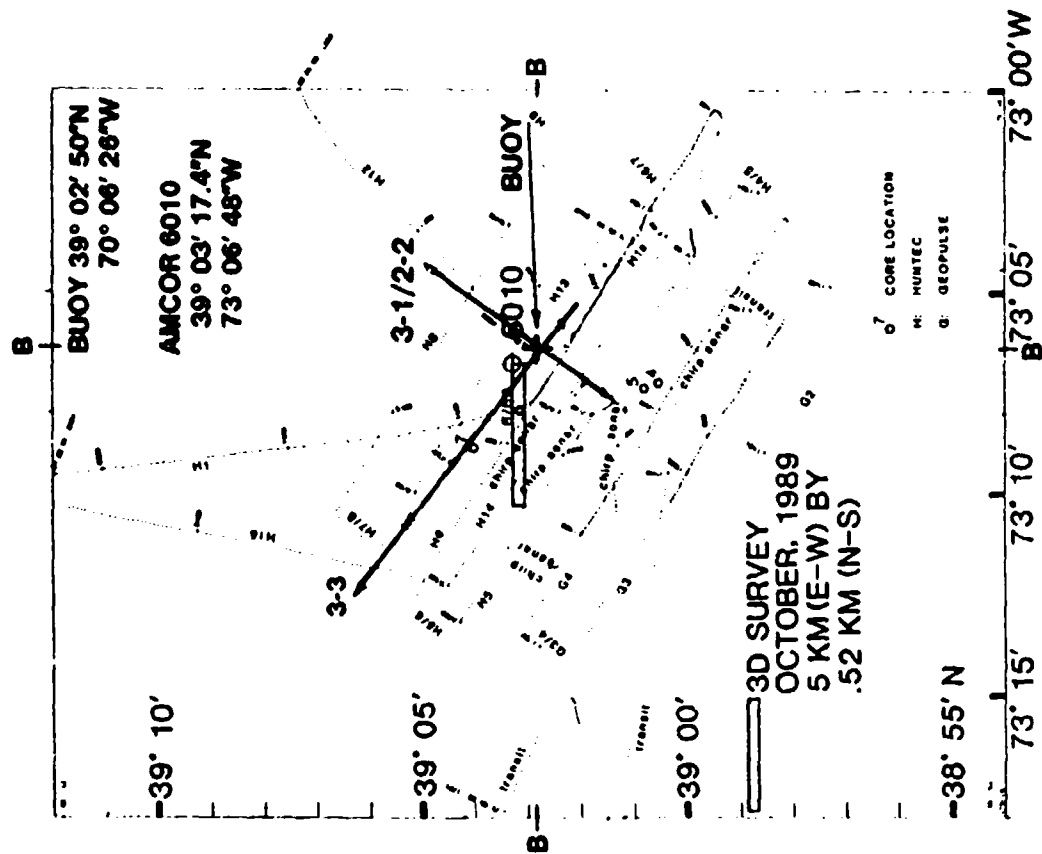
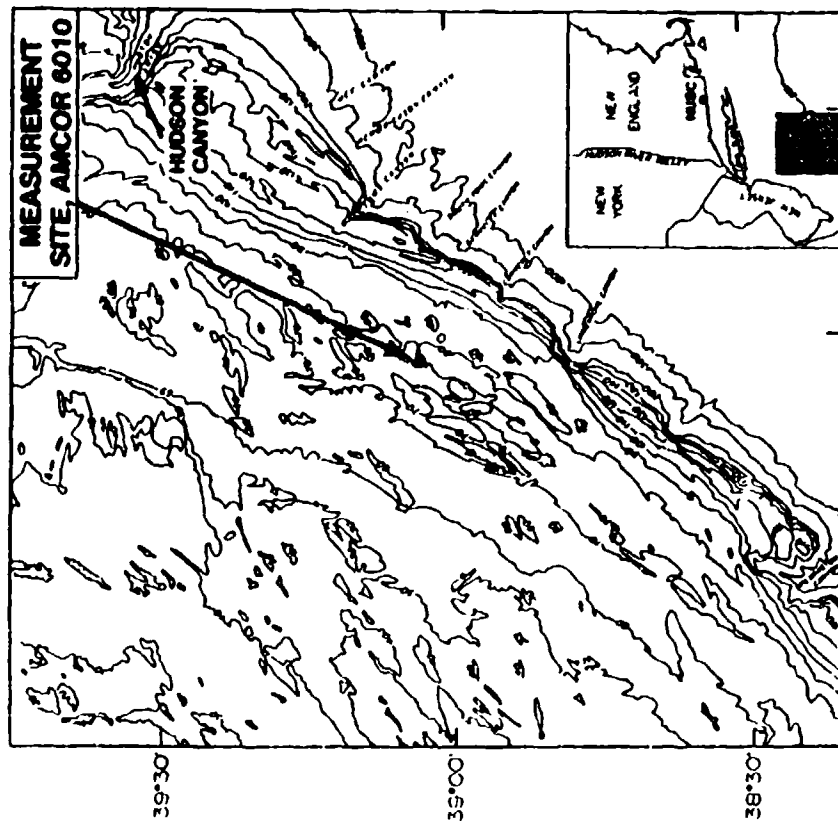
A handwritten signature in dark ink, appearing to read "M. J. Mayer", written over the typed name and title.

M. J. MAYER  
CAPTAIN, USN  
ASSISTANT DIRECTOR  
OFFICE OF BUDGET AND REPORTS

# VIEWGRAPH 3: THE EXPERIMENTAL AREA

HUNTEC 3-D SURVEY - J. AUSTIN et al.

NEW JERSEY  
CONTINENTAL SHELF  
HUDSON CANYON EXPERIMENT



### Viewgraph 3 The Experimental Area

This viewgraph shows the general location of the experimental area. Part (A) shows the locale on the east coast with respect to the Hudson Canyon and NUSC (NUWC-NL). Part (B) shows the experimental tracks in relation to the geopulse and Hunttec surveys conducted by the Woods Hole Oceanographic Institution and the University of Texas at Austin. Our particular tracks were based on preexperiment discussions with John Ewing and John Milleman of WHOI. One set of tracks was designed to parallel the shelf (TL 2-2/3-1), the other, to proceed perpendicular to the shelf (TL3-3). The tracks were run at constant RPM operation between selected waypoints:

RUN	WAYPOINT 1	WAYPOINT 2
TL2-2	39° 01.2'N 73° 08.0'W	39°04.3'N, 73° 04.9'W
TL3-1	39° 02.75'N, 73° 06.5'W	39° 05.1'N, 73° 04.1'W
TL3-3	39° 02.75'N, 73° 06.5'W	39° 11.8'N, 73° 21.9'W

Additional tracks were made but are not the subject of this paper. The actual tracks differ, as you can observe, from the tracks used by Milliman. The reason for this difference was our desire to have a rather flat propagation track as well as a sloping one. A brief site survey was run shortly after we arrived at the AMCOR site and the waypoints and tracks chosen.

Accession For	
NTIS GRA&I	<input checked="checked" type="checkbox"/>
DTIC TAB	<input type="checkbox"/>
Unannounced	<input type="checkbox"/>
Justification	
By _____	
Distribution/	
Availability Codes	
Dist	Avail and/or Special
A-1	



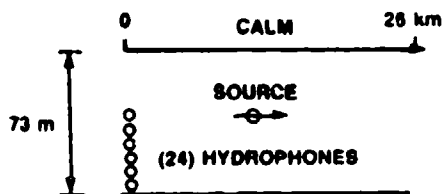
## Viewgraph 4 The Experiment

This viewgraph is a schematic of the experiment and the values shown are nominal but accurate. The basic experiment was to measure calibrated sound transmissions such that both TL and horizontal wavenumber spectra could be determined. Flat and sloping cases were studied. Oceanographic and bathymetric data were also obtained in order that we could compare our results with both range-independent and dependent calculations. The experiment required a calm sea state for two reasons: (a) sea surface spectra were not measured and (b) our vertical array only had one depth gauge by which tilt could be determined. Although we had some days with rough seas, the data discussed in this paper was taken when the sea was flat.

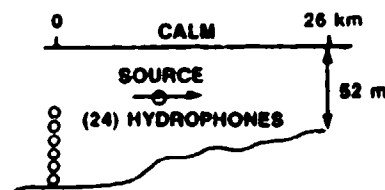
# HUDSON CANYON EXPERIMENT

## ● TWO BASIC CASES:

### 'A' UNIFORM DEPTH



### 'B' VARYING DEPTH



## ● EXPERIMENTAL PARAMETERS

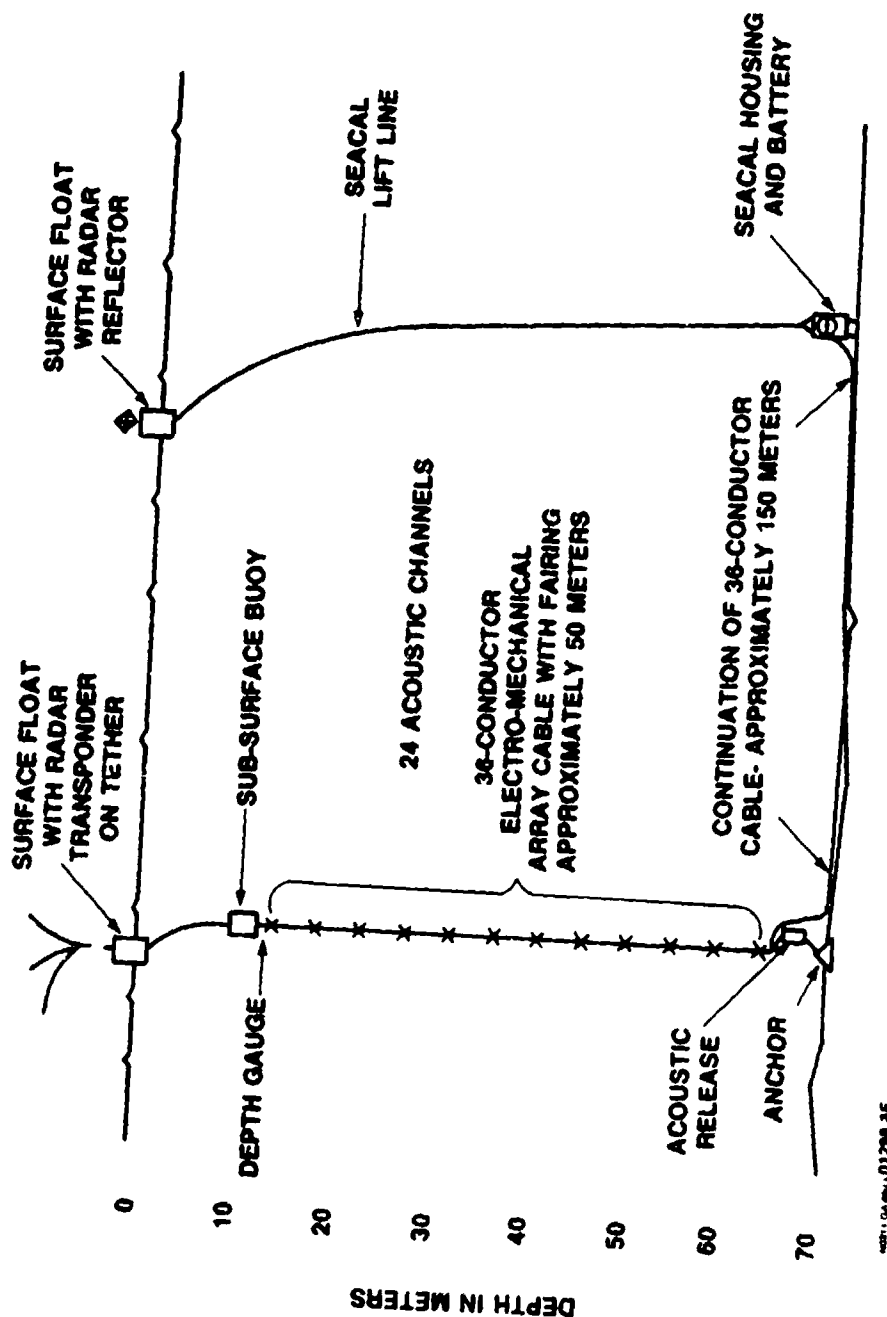
WATER DEPTH:	'A' 73 m, 'B' 73 m → 52 m
RANGES:	0-4 km, 0-26 km
SEA STATE:	< BEAUFORT 2
OCEANOGRAPHIC COND.:	STABLE APPEARANCE, VARIABLE SVP
FREQUENCIES:	50-75-175-275-375-525-600 Hz
SOURCE DEPTH:	36 AND 50 m
SPEED:	CONTS. MIN. RPM (2 AND 5 kts)
RECEIVER DEPTHS:	24 CHANNELS- SPACED 2.5 m- "UP FROM BOTTOM"

## ● BASIC MEASUREMENTS UNDER CALM SEA STATE CONDITIONS

- CALIBRATED PROPAGATION LOSS VS RANGE
- OCEANOGRAPHIC DATA - BATHYMETRY
- HORIZONTAL WAVENUMBER SPECTRA - 4 km AND 26 km

**THIS PAGE INTENTIONALLY LEFT BLANK**

# HUDSON CANYON EXPERIMENT ACOUSTIC MEASUREMENTS



VIEWGRAPH 5

## Viewgraph 5 The Receiver System

This viewgraph shows the configuration of the receiving array and SEACAL measurement systems. This system consisted of a sparbuoy (12 m (40 ft), 4.9 m (16 ft) above surface) with a radar transponder (Del NORTE), a 7.62 m (25 ft) tether, a subsurface buoy (700 lbs of buoyancy), a pressure transducer, 24 (Bentnos AQ-17) hydrophones mounted on a "hair" faired cable with 2.5-m spacing, an acoustic release, and an 1800-lb "Railroad - Wheel" anchor. The pressure vessel and electronics (the SEACAL) were located approximately 150 m from the anchor. These were connected by a 3/8-in. double braided lift line to a surface float with a radar reflector. Thus, this arrangement permitted the lifting, removal, reconditioning and replacement of the SEACAL system without moving the array.

Although the subsurface buoy had sufficient buoyancy force to keep the array vertical, the mismatch created by the length of the system between the anchor and sparbuoy (78 m) and the water depth (73 m) resulted in a range bias between 5-11 m, depending on the sea state. The uncertainty in range due to the radar transponder was determined by at-sea and shore calibrations to be  $\pm 2$  m.

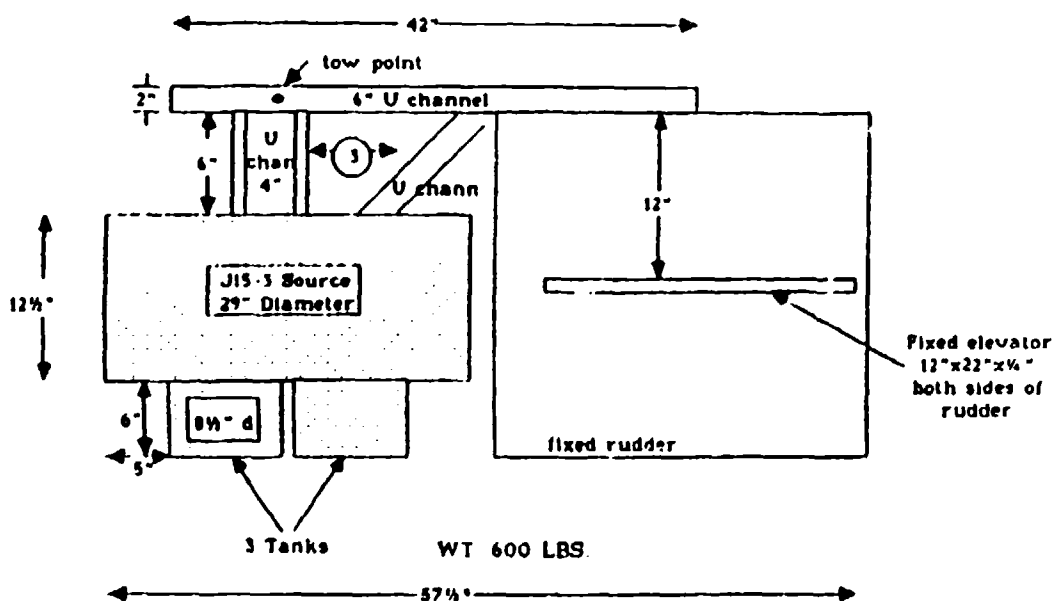
The SEACAL system is a 27-channel data acquisition system and utilizes two standard VHS tape recorders to record up to 10 gigabytes of data over either a standard record of 8 hours or a slow recording mode of 16 hours. The system was configured for this test to acquire data from 24 (AQ-17) hydrophone channels, a depth gauge and a reference clock. Each hydrophone channel had its own signal conditioning consisting of an AQ-17 hydrophone, preamplifier, 0 dB gain buffer amplifier, preemphasis (-6 dB/octave from 1 kHz), a variable gain amplifier (0-48, 50-98 dB in 6 dB steps), an 8-pole Tchebychev antialiasing filter, a sample and hold followed by a 14-bit analog to digital converter (AID) with a 3263.4 Hz sample rate. All channels are sampled simultaneously preserving channel-to-channel phase information. Each channel's data sample is enabled on the data bus in sequence resulting in a bus data rate of 88,112 Hz. Digital words containing the depth, time code, and synchronization data are interleaved with the acoustic data by the control timing board, creating a fixed repeating sequence. This timing-and-control circuit controls all AID rates and rates synchronously from the 88,112 Hz word-rate clock of the video.

The AQ-17 hydrophones were chosen because their frequency response is flat between 10 and 1 kHz. Hydrophones were calibrated at the NRL/USRD and recalibrated at the NUWC Dodge Pond facility. The mean hydrophone sensitivity was  $-174.3$  dBV/ $\mu$ Pa  $\pm 0.4$ .

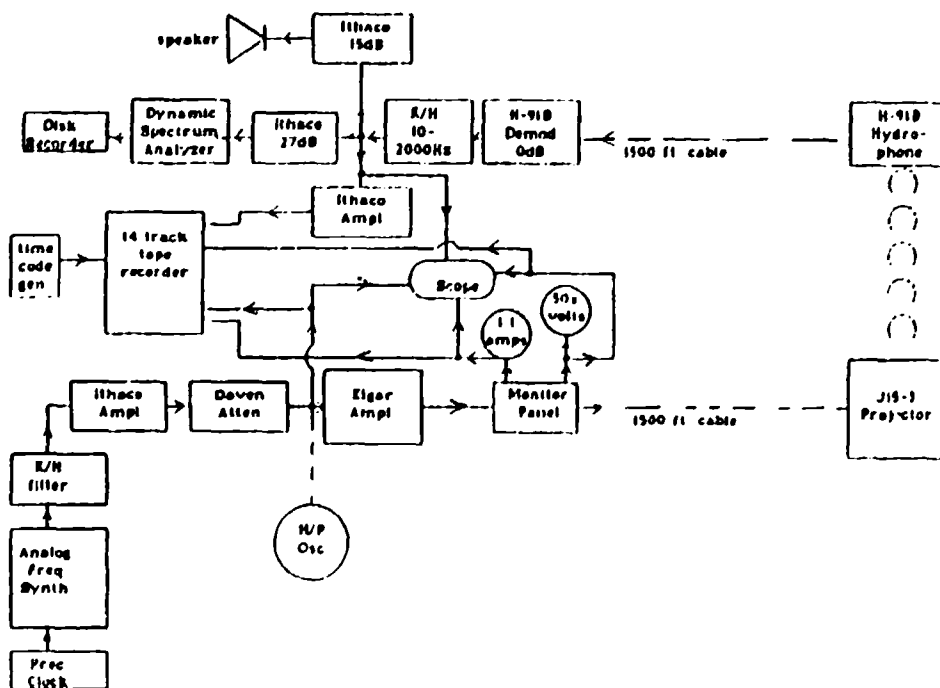
## Hydrophone Locations And Height Off Bottom

HYD No.	S/N	HS dBV/ $\mu$ Pa	Height Off Bottom (m)	D (m)
1	177	-174.0	58.5	14.95
2	172	-174.0	55.55	17.45
3	173	-175.6	53.05	19.95
4	174	-174.0	50.55	27.45
5	175	-174.0	48.05	24.95
6	176	-174.4	45.55	27.45
7	178	-174.6	43.05	29.95
8	179	-174.6	40.55	32.45
9	180	-174.1	38.05	34.95
10	182	-174.4	35.55	37.45
11	183	-174.6	33.05	39.95
12	185	-174.0	30.55	42.45
13	186	-174.2	28.05	44.95
14	187	-174.4	25.55	47.45
15	188	-174.0	23.05	49.95
16	189	-174.0	20.55	52.45
17	190	-174.0	18.05	54.95
18	191	-174.2	15.55	57.45
19	192	-174.0	13.05	59.95
20	193	-174.4	10.55	62.45
21	194	-175.0	8.05	64.95
22	195	-173.6	5.55	67.45
23	196	-174	3.05	69.95
24	197	-174.4	0.55	72.45
		-174.3 $\pm$ .4		
		dBV/ $\mu$ Pam		

THIS PAGE INTENTIONALLY LEFT BLANK



Sound Source J15-3A in Tow Body



Block Diagram of Data Acquisition System

## VIEWGRAPH 6: THE SOUND SOURCE

## **Viewgraph 6 The Sound Source**

The sound source used in this experiment was a USRD type J15-3, consisting of three moving-coil-driven rubber diaphragms. This transducer was capable of operating in the 50 to 600 Hz range with levels of 165 dB//1  $\mu$ Pa/1m. (Transmit current response 164 dB//1  $\mu$ Pa/1A/1m and voltage 123 dB//1  $\mu$ Pa/1V/1m @ 50 Hz.) The source was mounted to a frame with a fin stabilizer. A calibrated hydrophone (USRD-H91) was attached to the source with a 2-meter flexible cable and was used to monitor the source level. In addition, monitoring of the drive amplifier voltage and current provided an additional check on the transmitted level. This viewgraph shows a schematic of the source tow body and the source data acquisition system. The J15-3 and H91 monitor were calibrated at the NUWC Dodge Pond facility to ensure the integrity of the NRL/URD calibrations.

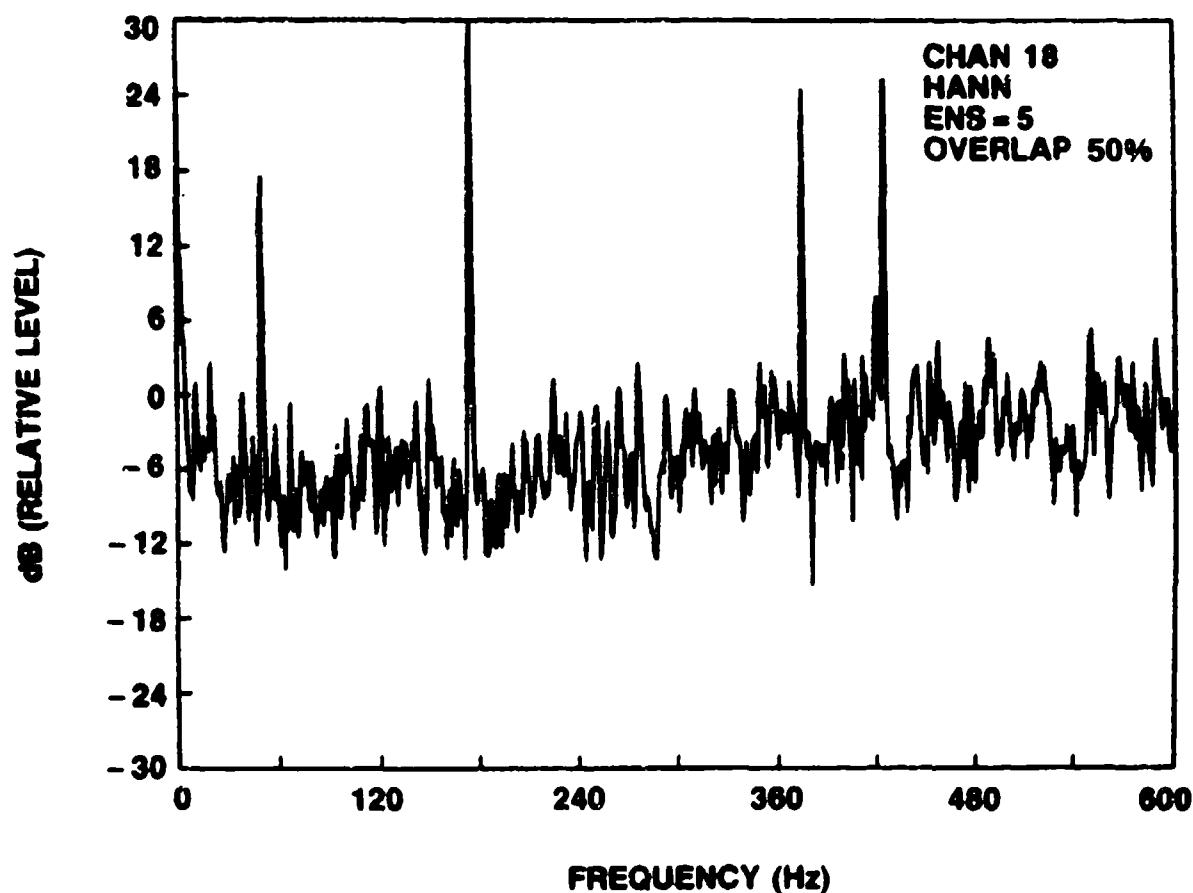


## Viewgraph 7 Sound Source Spectrum

This viewgraph shows an example of the transmitted tones from our F9 sequence (50-175-375-425 Hz) as received on hydrophone 18 of the SEACAL measurement system.

Two tone sequences were used for the data presented here, the second, not shown, was F8 (75-275-525-600 Hz). The four tones from the F9 sequence shown in this viewgraph illustrate the high signal-to-noise ratios obtained in our 4 km runs.

### HUDSON CANYON EXPERIMENT SEPT 88



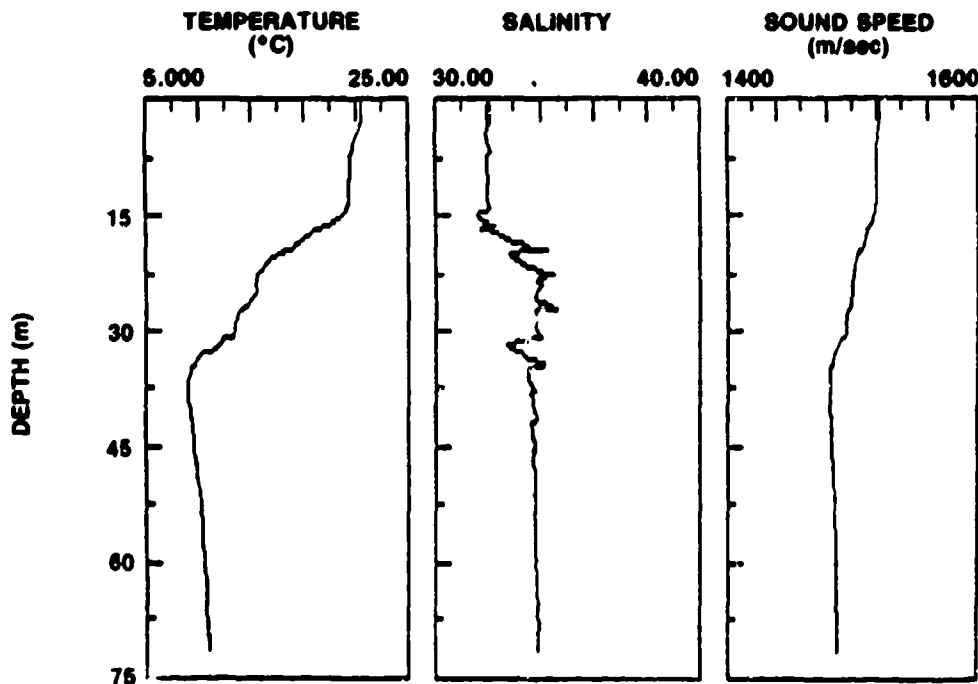
RECEIVED SIGNAL LEVEL (dB) VERSUS FREQUENCY FOR TEST 6 (TL#2-2). THESE DATA SHOW HIGH SIGNAL-TO-NOISE RATIOS FOR THIS RUN.

0011 00000 01200 00

## Viewgraph 8 Sound Velocity

During the course of this experiment, conductivity, temperature and sound-speed-versus-depth measurements were made. Two measurement devices were utilized, the SEABIRD CTD and the Applied Micro Systems SVP. The CTD data were used with Wilson's equation to determine sound-speed-versus-depth profiles. The SVP measurement employed a sonic velocimeter. Simultaneous measurements enable the comparison of both measured and computed SVP. The problem encountered with these measurements was the necessity of stopping the research vessel, USS Ranger, hence measurements were made at turning points of our measurements and at a few selected times during the course of the transmission runs. This resulted in a sparse sampling of the environment, sparser than one would like for a coastal environment. Examination of these profiles shown in this viewgraph illustrates the problem. The sound velocity profile shows an isovelocity layer (1520 m/sec) to a depth of 15 meters and a decrease at the rate of  $\partial C/\partial D \sim 1.5 \text{ sec}^{-1}$  to a depth of 35 meters allowed by another isovelocity layer (1487 m/sec). The thermocline region also shows salinity variations. Examination of the other SVP/CTD data shows a combined spatial and temporal variability in this 15-36 m region, which is an important factor to be considered in these transmission studies.

## HUDSON CANYON EXPERIMENT SEPT 88

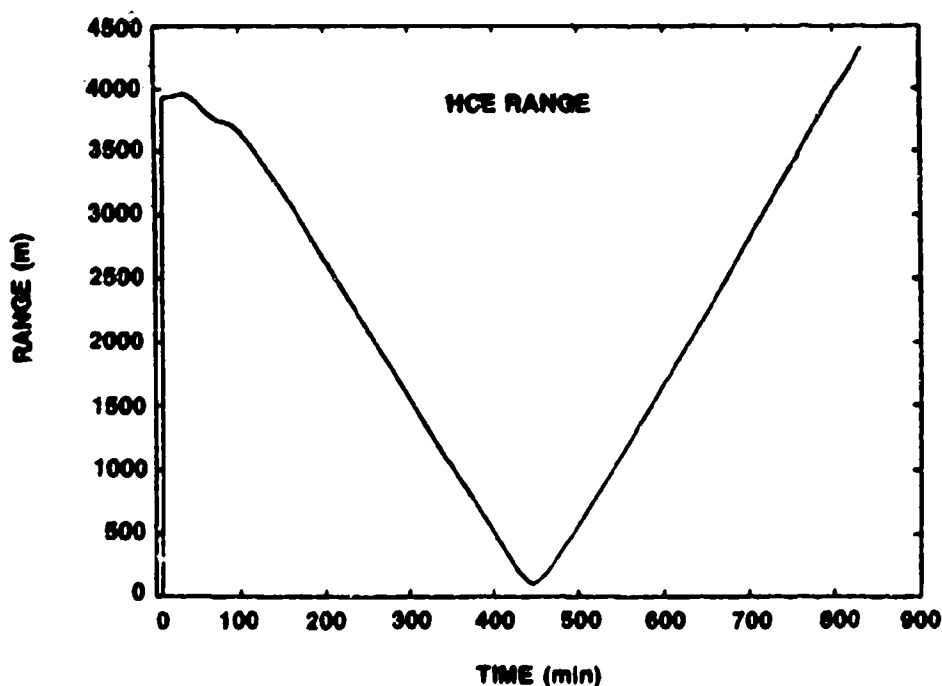


TEMPERATURE, SALINITY, AND SOUND SPEED VERSUS DEPTH. THESE DATA ARE REPRESENTATIVE OF THE OCEANOGRAPHIC DATA FOR TEST 6 (TL#2-2).

### Viewgraph 9 TL202, Range Versus Time

The experiment was designed to be conducted at a constant speed. This was accomplished by working closely with the ship's captain. Two basic types of runs were conducted. The slower speed run shown on this viewgraph ( $\sim 1.835$  m/sec) was conducted by selecting remote locations, referred to as "waypoints," at opposite extremes with the buoy as the marker for CPA. This enabled a true course to be maintained. The speed was controlled by running the ship's power plant at constant minimum RPM. The slow speed was accomplished by single propeller operation and by clutching in and out on a timed schedule. The longer, higher ship's speed runs were single propeller constant RPM runs. Due to the low sea states, lack of strong winds, and currents, we were able to maintain fairly steady tracks and speed. Since the mean sonic speed is 1497 m/sec this corresponds to a Doppler shift of  $1.23 \times 10^{-3} f_0$  or  $\pm 6.14 \times 10^{-2}$  Hz for 50 Hz and  $9.02 \times 10^{-2}$  Hz at 75 Hz. By trial and error we were able to keep our CPA on the order of 100 m.

## HUDSON CANYON EXPERIMENT SEPT 88



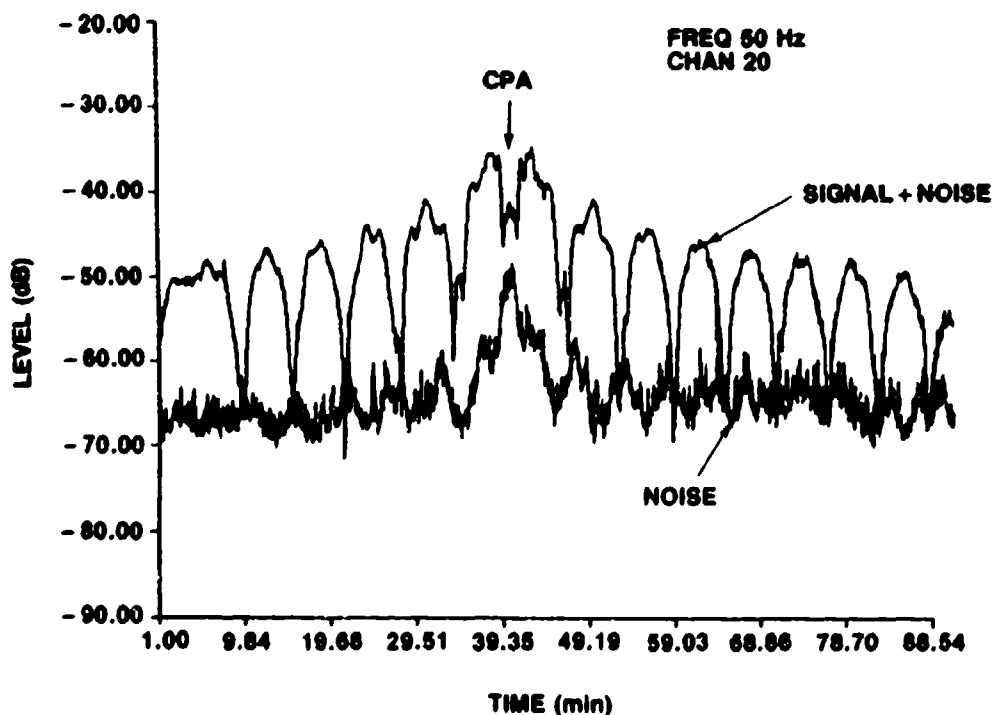
RADAR TRANSPONDER RANGE VERSUS RUN TIME FOR TEST 6 (TL#2-2). THIS LINEARITY OF RANGE WITH TIME INDICATES HIGH RESOLUTION SYNTHETIC APERTURE PROCESSING IS FEASIBLE.

NOV 1 04:22:01 1988

## Viewgraph 10 Signal Plus Noise Versus Time TL2-2

Shown on this viewgraph is the signal-plus-noise and noise levels corresponding to the previous range-versus-time curve. The data shown here were processed at sea with a double-Hann-shaded, 1024-point, Fourier transform approximately 1/3-seconds long. The origin of the graph represents the start of the constant speed run. In this case, the propeller was clutched "in" and "out" on a regular interval, and the result of this operation is shown on the noise curve. The signal-to-noise curve illustrates the high signal-to-noise rates and a pronounced model interference pattern. This pattern is what one expects from two modes of equal amplitude and a smaller amplitude third mode at short ranges. These results, when merged with the range-versus-time data, form the basis for synthetic aperture processing.

### HUDSON CANYON EXPERIMENT SEPT 88



RECEIVED SIGNAL LEVEL (dB) AND NOISE LEVEL (dB) VERSUS TIME FOR TEST 6 (TL#2-2). THESE DATA WHEN MERGED WITH THE RANGE DATA FROM FIGURE 1 WILL YIELD RECEIVED SIGNAL LEVEL VERSUS RANGE. THE SYMMETRIC PATTERN, HIGH SIGNAL-TO-NOISE RATIO, AND DISTINCT MODEL INTERFERENCE PATTERN INDICATE A HIGH QUALITY DATA SET.

01200.78

## **Viewgraphs 11, 12 and 13 The Synthetic Aperture and High Resolution Doppler Techniques**

A prime purpose of this experiment was to investigate the utility of the Fourier-Hankel Technique (Frisk [1984]) and high resolution Doppler processing such as employed by Glattetre (1989) to estimate the horizontal wave number spectrum. Shown on these three viewgraphs is the mathematical outline of each approach, which differ in the practical implementation.

The "quadrature" approach employed by Frisk (1984) generates a complex pressure series for a slowly moving source. This technique allows one to continuously adjust the reference frequency, thereby compensating for frequency mismatch. However this technique requires precise position-versus-time data.

The sequential Fourier transform technique, sequential phase-corrected Fourier transforms, is similar to the synthetic-aperture processing employed by Yen and Carey (1989). This technique may be used at higher relative speeds, provided the time sample for each Fourier transform is short, the range smearing small, and the frequency and timing errors can be controlled.

The high resolution Doppler technique can be performed at higher relative speeds, but the motion must be constant and the relative separation between the source and receiver must be known. In particular, this technique holds promise for those applications using a towed array.

It is easily shown that the "quadrature" and "Fourier" technique produce a biased estimate of the wavenumber, that is, a shifted horizontal wavenumber spectra. Of course, this bias may be eliminated by precise knowledge of the motion or by reducing the relative speed.

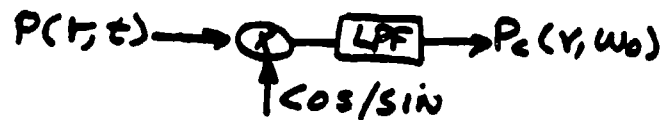
Finally, I show the relationship between the HRD approach and the Fourier-Hankel transform. The importance of the  $\sqrt{v}$  term is that of an amplitude shading characteristic that can be ignored if only the wavenumber characterization is required.

# SYNTHETIC APERTURES

## THREE TECHNIQUES

### FRISK-LYNCH-RAJAN

'QUADRATURE'  $P_c(r, \omega_0) = \int_{\Delta T} [\cos \omega_0 t + j \sin(\omega_0 t)] P(r, t) dt$



'HANKEL'

$$P(k, \omega_0) = \int_0^{R_m} P_c(r, \omega_0) e^{ikr} \frac{\sqrt{r}}{\sqrt{k}} dr$$

### SEQUENTIAL 'FOURIER/HANKEL'

'FOURIER'  $P(r, \omega) = \int_{-\Delta t/2}^{\Delta t/2} P(r, t) e^{-i\omega t} dt$

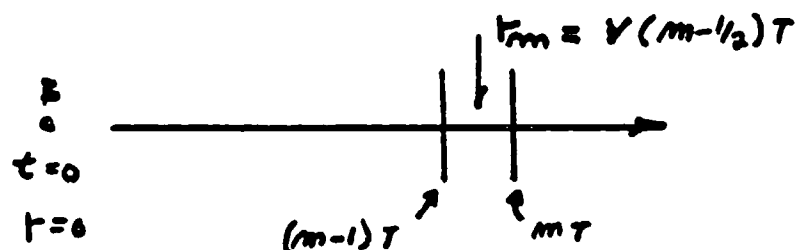
'HANKEL'  $P(k, \omega) = \sum_{m=1}^N P(r_m, \omega) e^{ikr_m} \frac{\sqrt{r_m}}{\sqrt{k}} \Delta r_m$

### HIGH RESOLUTION DOPPLER

$$P(\omega) = \int_0^{T_{max}} P(r, t) e^{-i\omega t} dt$$

## THE PEKERIS WAVEGUIDE MODEL

$$P(r,t) = \frac{\rho \omega \sqrt{8\pi}}{H} \sum_{m=1}^{\infty} P(\beta_m, k_m, d, z) \cos(\omega_0 t - k_m r + \pi/4) / \sqrt{F}$$



FOR THE  $n^{\text{th}}$  MODE

$$P_{0mm} = \int_{(m-1)T}^{mT} \frac{\cos(\omega_0 t - k_m r + \pi/4)}{\sqrt{F}} e^{-i\omega t} dt P_0$$

AND

$$P_m(k, \omega) = \int_0^{R_m} P_{0mm}(t_m, \omega) e^{ikr} r dr$$

THE RESULT

$$P_{0m}(k, \omega) = C G(k_{0m}) \sin(\beta_{0m} d) \sin(\beta_{0m} z) \frac{\sin[MVT(R - k_{0m} - \frac{\Delta\omega}{V})/2]}{\sin[VT(k - k_{0m} - \frac{\Delta\omega}{V})/2]}$$

$$P_{0m}(k, \omega) \text{ PEAKS AT } k = k_{0m} + \frac{\Delta\omega}{V} !$$

A BIASED ESTIMATE !

## THE FOURIER-HANKEL TRANSFORM

$$P(k, \omega) = \int_0^{R_{\max}} e^{ikr} r dr \int_0^T e^{-i\omega t} dt [P(r, t)] .$$

PEKERIS

$$P(r, t) = \frac{\rho \omega \sqrt{gH}}{H} \sum_{n=1}^{\infty} P(\beta_n, k_n, d, z) \frac{\cos(\omega_0 t - k_n r + \pi/4)}{\sqrt{r}}$$

WHEN  $\dot{\phi}(t) = \omega_0 - k_{0n} r \neq \omega_0$  THE TIME AND  
 $r$  INTEGRALS CAN BE DONE INDEPENDENTLY.

$$\text{WHEN } \dot{\phi}(t) = \omega_0 \left( 1 \pm \frac{v}{c_m} \right) = \omega_0 \left( 1 \pm \frac{v}{c} \cos \theta_n \right) = \omega_{dn}$$

THEN THE FOURIER-HANKEL TRANSFORM BECOMES

$$P(\omega) = \int_0^T e^{-i\omega t} dt [\sqrt{v\epsilon} P(r, t)]$$

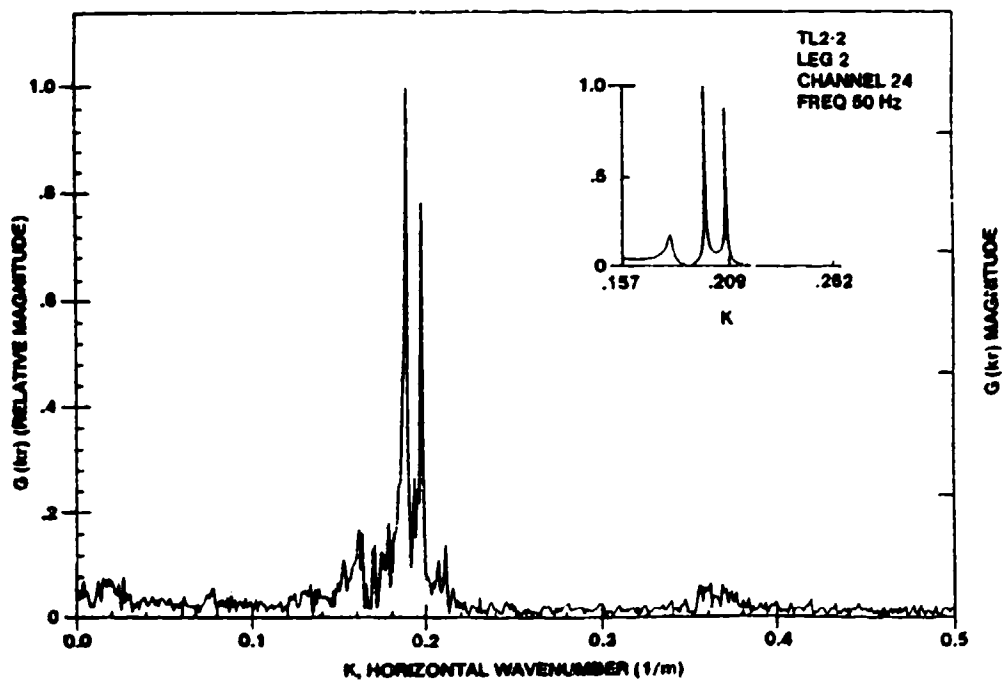
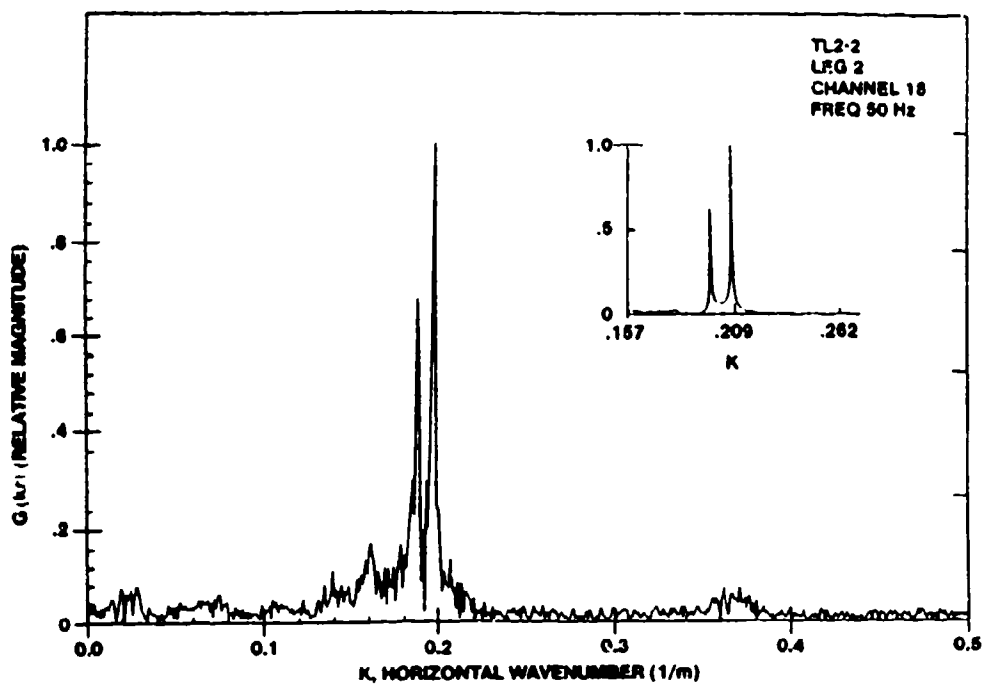
AND THIS IS THE FOURIER TRANSFORM OF

$$\text{OF } [\sqrt{r} = \sqrt{v\epsilon}] \text{ TIMES } P(r, t)$$

THE HIGH RESOLUTION DOPPLER APPROACH DROPS  
 THE  $\sqrt{r}$

$$P(\omega) = \int_0^T e^{-i\omega t} p(r, t) dt \quad \omega_d = \omega_0 \left( 1 \pm \frac{v}{c} \cos \theta_n \right)$$





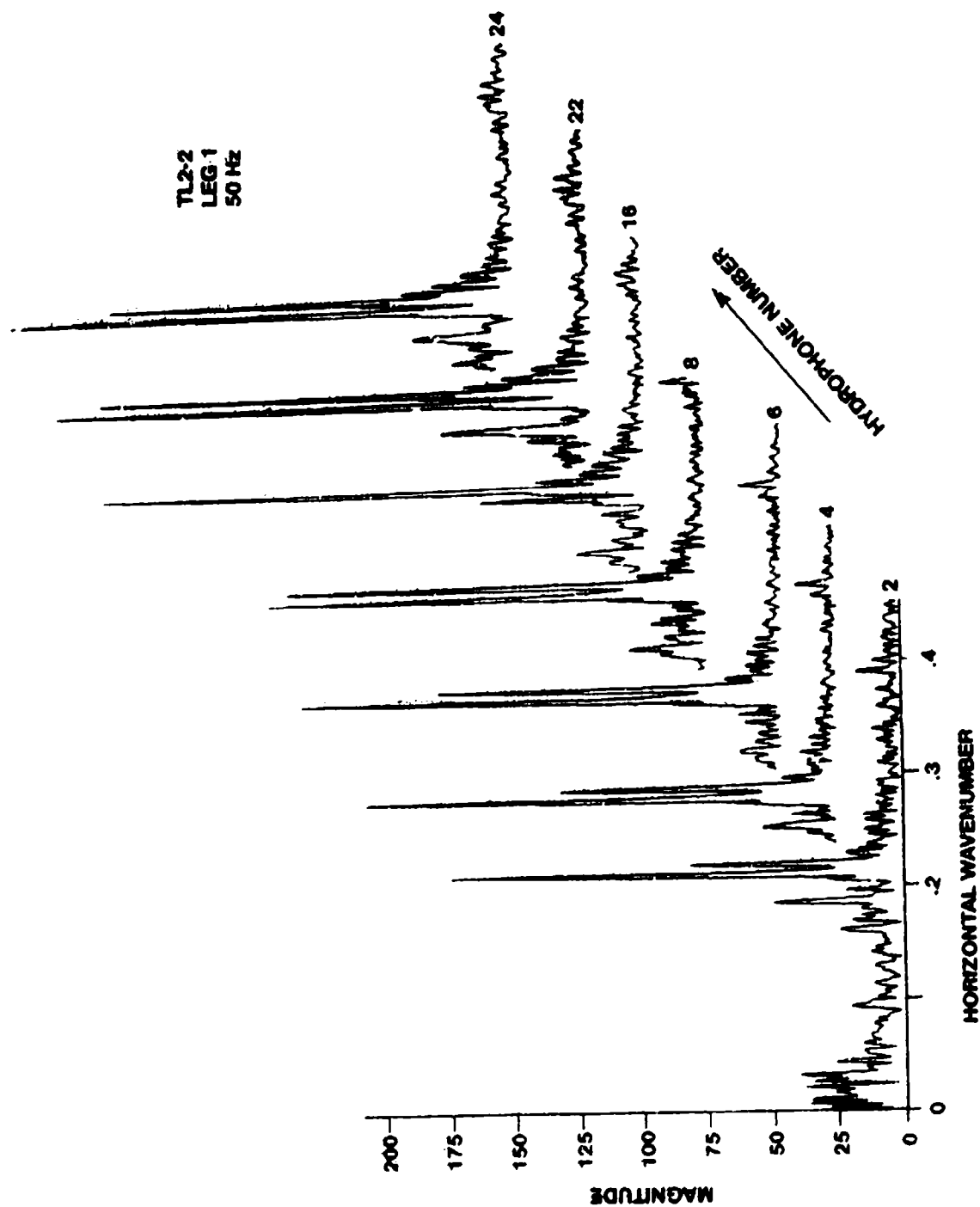
VIEWGRAPH 14

### Viewgraph 14 Measured Horizontal Wavenumber Spectra

TL 2-2, legs 1, 2, and 3 were transmission tests specifically conducted to measure the horizontal wavenumber spectrum. Shown on this viewgraph are the linear horizontal wavenumber spectra for 50 Hz and hydrophones numbered 18 and 24. Also shown are the results of calculations performed with SAFARI, using a simplified critical angle bottom without shear. These spectra are plotted relative to the highest mode, but also scale relative to one another. Qualitatively the calculations and model results agree.

	18 Meas.		18 Cal.		24 Meas.		24 Cal.		
	RM	%	%		K	RM	%	%	K
1.		11	100	100	.1987	9.6	100	100	.1975
2.		7.4	67	34	.1886	12.2	127	114	.1895
3.		1.45	16.5	7.5	.1623	2.1	20.8	18.2	.160

The largest disagreement was in the estimates of the horizontal wavenumber. These biased wavenumbers showed complimentary shifts for legs 1 and 2. These bias errors are due to (a) Doppler, (b) frequency mismatch and (c) measurement timing errors. Performing a higher resolution Fourier transform changes the bias. However, we have these spectra as a function of depth, and we also have an independent measure of average sound speed.



VIEWGRAPH 15

### Viewgraph 15 Linear Horizontal Wavenumber Spectra Versus Hydrophone Number

The sequence of wavenumber spectra clearly shows the modal amplitude dependence as a function of depth. Here we show the spectra for the even numbered hydrophones. This case of propagation in a 73 m waveguide at 50 Hz clearly shows three modes. This depth variation in modal amplitudes enables the determination of the vertical wavenumber. Although we have chosen the Pekeris Waveguide as our model of sound transmission, the actual measured case has a variation in sonic speed with depth.

Since  $k = k_w \sin(\theta)$  and according to Snell's law

$$\frac{\sin\theta(z)}{C(z)} = \text{CONSTANT}$$

further, since  $k_w^2 = k^2 + \beta_v^2$ , where  $k_w$  is the water wavenumber and  $\beta_v$  is the vertical wavenumber, we have at each depth,

$$k_w(z)^2 = \beta_v(z)^2 + k^2,$$

$$k^2 \cdot z = \int_0^z k^2 dz = \int_0^z k_w^2 dz - \int_0^z \beta_v(z)^2 dz,$$

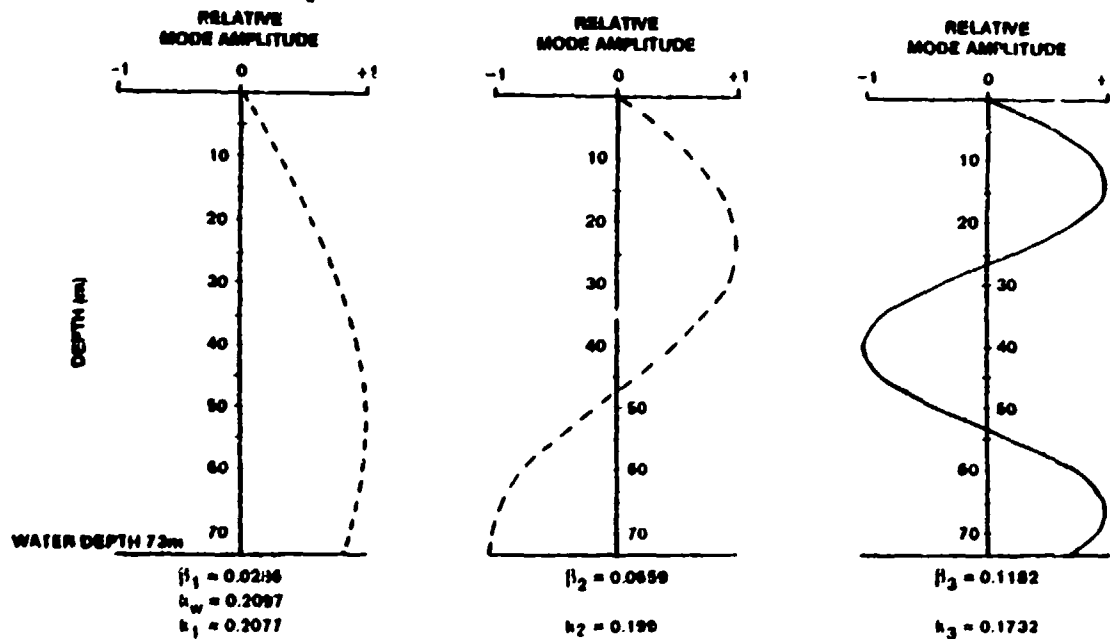
$$k^2 = \left(\frac{1}{z}\right) \int_0^z k_w^2 dz - \left(\frac{1}{z}\right) \int_0^z \beta_v(z)^2 dz.$$

Now each integral represents the mean square value of the water and vertical wavenumbers. If we assume  $\overline{k_w^2} = \overline{k_w^2}$  then we have

$$k^2 = (\overline{k_w})^2 - (\overline{\beta_v})^2.$$

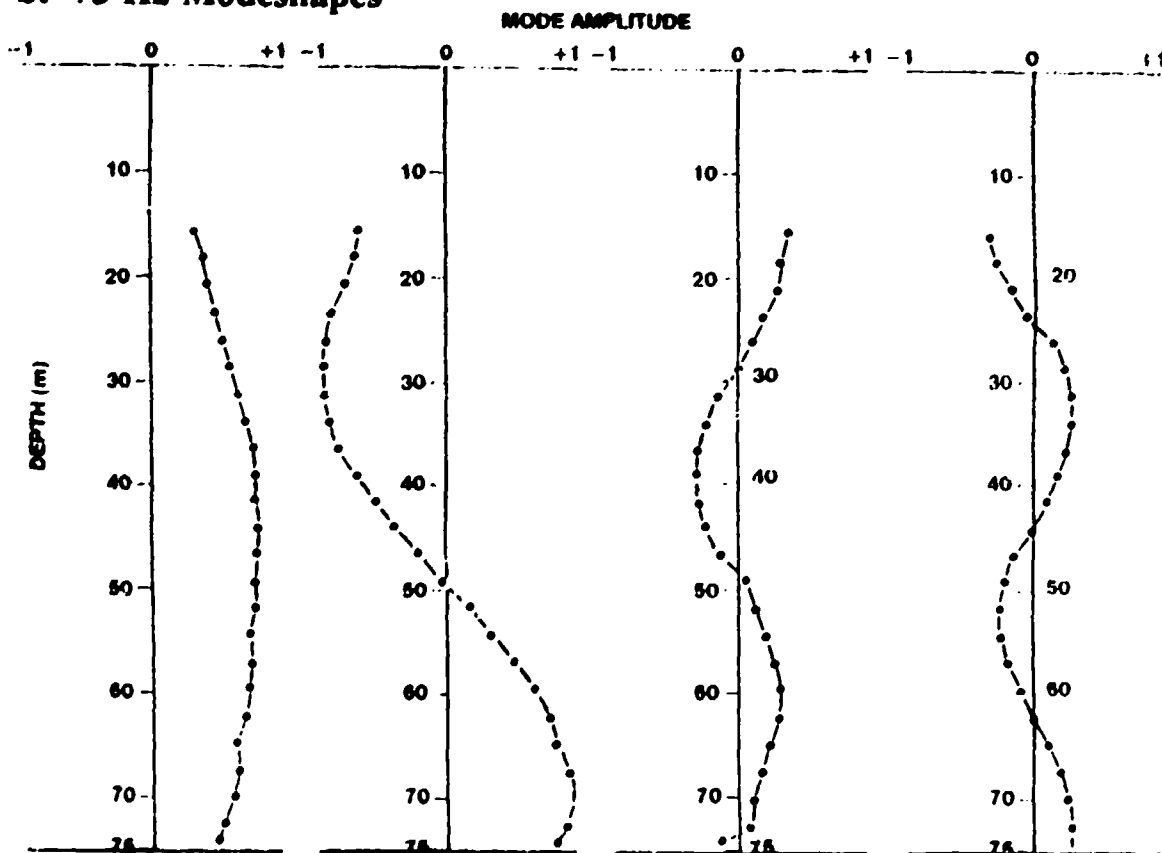
Since we measure the sonic speed variation in the water, we know the frequency, the quantity  $\overline{\beta_v}$  can be determined by the depth variation of the modal peaks, a refined estimate of  $k$  can be made.

### a. 50 Hz Modeshapes



MODE SHAPES CALCULATED FROM  $\beta$  VALUES DETERMINED FROM MEASURED SPECTRAL AMPLITUDE  $G(\omega)$  AT A FREQUENCY OF 50 HZ AND SEVERAL DEPTHS.

### b. 75 Hz Modeshapes



VIEWGRAPH 16A

## Viewgraph 16A Mode Shapes at 50 and 75 Hz

The mode shapes at 50 Hz and 75 Hz, shown here, were obtained from the previously discussed horizontal wavenumber spectra versus depth. These data have not been corrected for scalloping losses or changes in hydrophone sensitivity.

The 50 Hz results were curve-fit by a VLMS (visual least mean square) as well as a simplex [NELDER-MEADE] algorithm. The results were very close with respect to both vertical and horizontal wavenumbers.

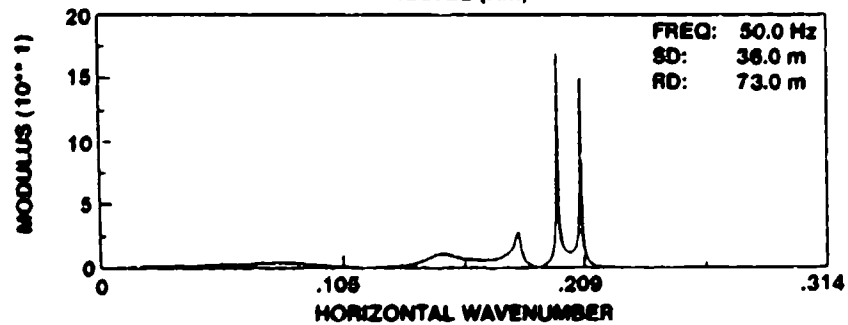
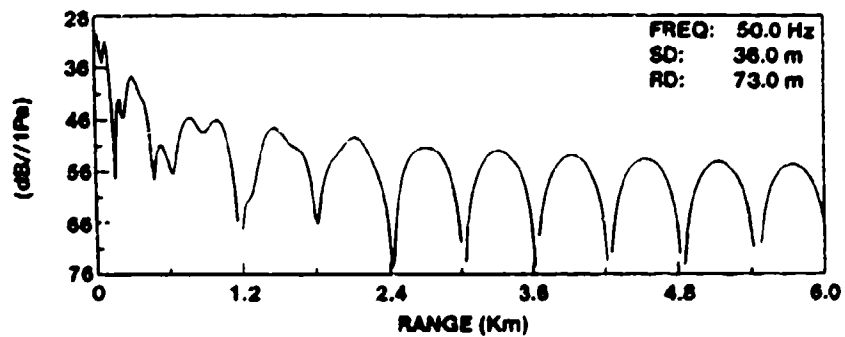
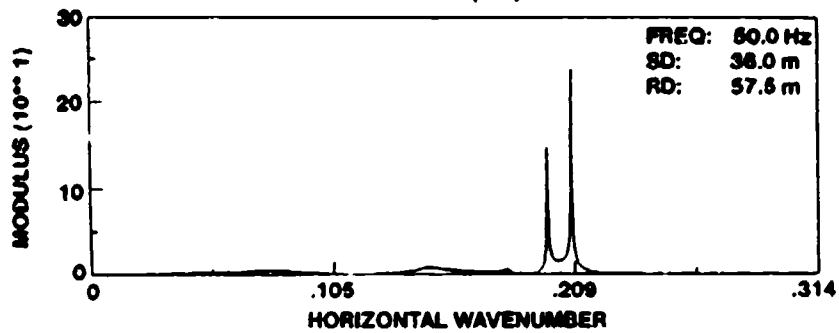
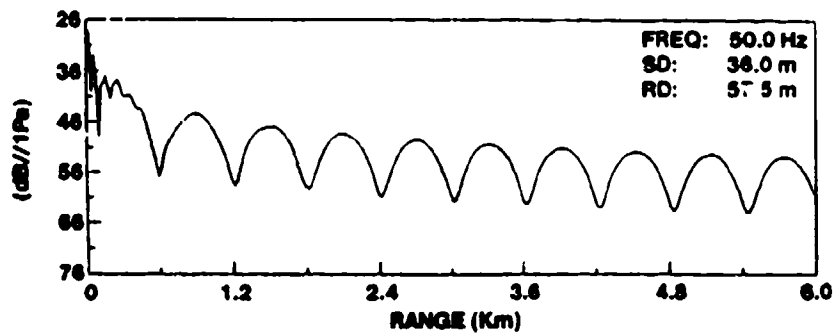
	1	2	3
$\beta_{vlms}$	0.0286	0.0659	0.1182
$\beta_v$	0.0290	0.0662	0.1201
$k_{h,lms}$	0.2077	0.199	0.1732
	0.2076	0.199	0.1719
$k_w = 0.2098$			

These results were obtained with the requirement that the pressure go to zero at the sea surface. Better fits can be obtained, however these fits do not correspond to this requirement. These results appear to be consistent from leg 1 to leg 2, provided one accounts for changes in water wavenumber.

Also shown are several modes for the 75 Hz data. These results were obtained two ways (a) high resolution Doppler and (b) horizontal wavenumber spectral estimates. The results are comparable but not exactly the same.

MODE		1	2	3
HRD	$\beta_v$	0.0433	0.0806	0.122
	k	0.312	0.0304	0.2899
HWNS	$\beta_v$	0.033	0.066	0.1346
	k	0.313	0.307	0.284
$k_w = 0.3147$				

The differences here are attributable to scalloping losses, that is, a loss of modal amplitude when the mode is between wavenumber bins or frequency bins.



VIEWGRAPH 16B

### Viewgraph 16B Safari Results

These SAFARI calculations were performed with a simulated bottom boundary condition, a step increase in density (2/1) and sonic speed (1487 to 1560) at the interface. This condition corresponds to a critical angle ( $\sim 28^\circ$ ) bottom loss characteristic. This set of calculations is shown to illustrate the character of the propagation. Calculations including the effects of shear were found to indicate little if any effect at these frequencies. The wavenumber from this boundary condition and geoacoustical modeling (Rogers) are shown below.

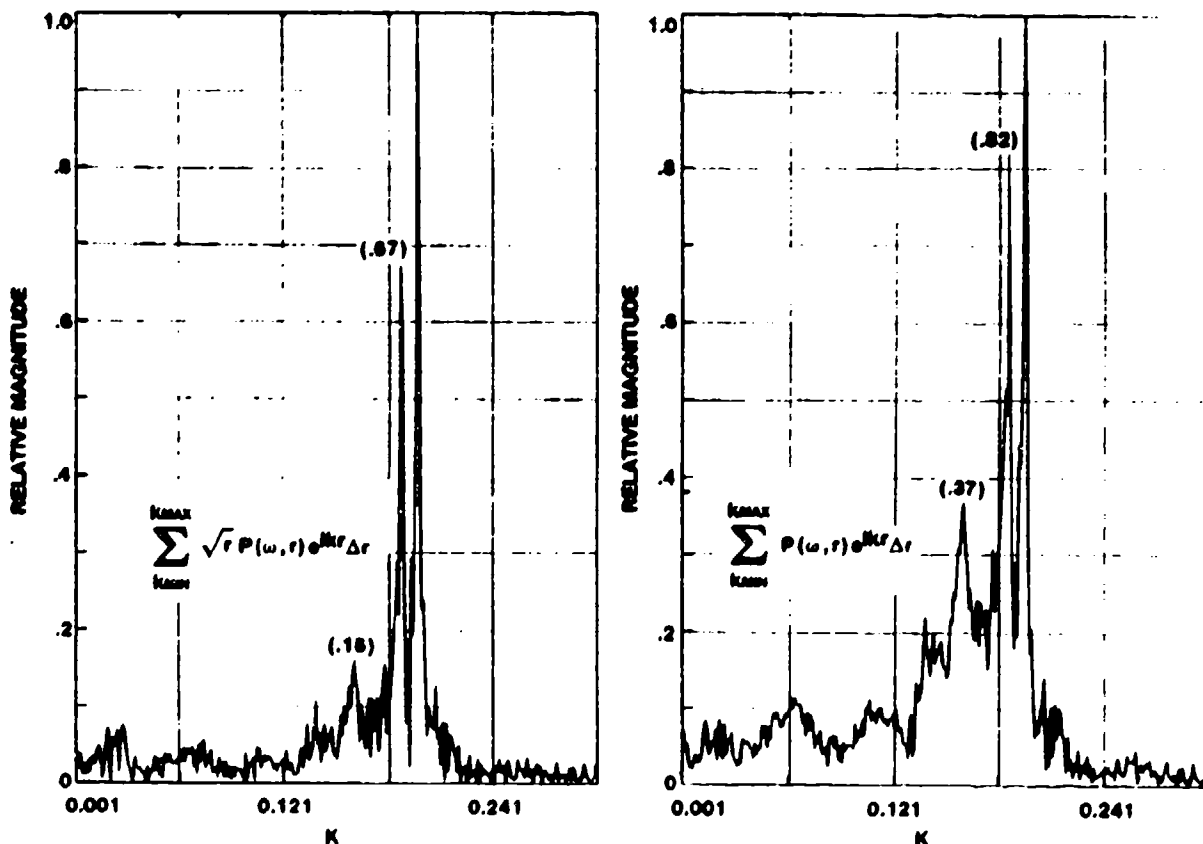
	SAFARI	ROGERS	RESULTS	SNAP
$k_1$	0.208	.2079	.2077	.2086
$k_2$	0.1978	.198	.199	.1989
$k_3$	0.1797	.184	.1732	.1824
				.1766

Notice the comparison between the wavenumbers places the uncertainty in the third significant digit. Variation of velocity profile and variation of water depth to simulate tidal effects results in a wavenumber variation of  $0 [\pm .009]$ . Parametric analysis was performed by Cederberg and others to determine these sensitivities and to estimate the basic uncertainties in these measurements. Three significant decimal places seem reasonable. Rogers employed a geoacoustic model based on sediment properties and Biot theory. He used an iterative scheme to determine modal attenuation factors and was able to achieve excellent agreement with these results and to estimate the attenuation factors.



## Viewgraph 17 The $\sqrt{r}$ Effect

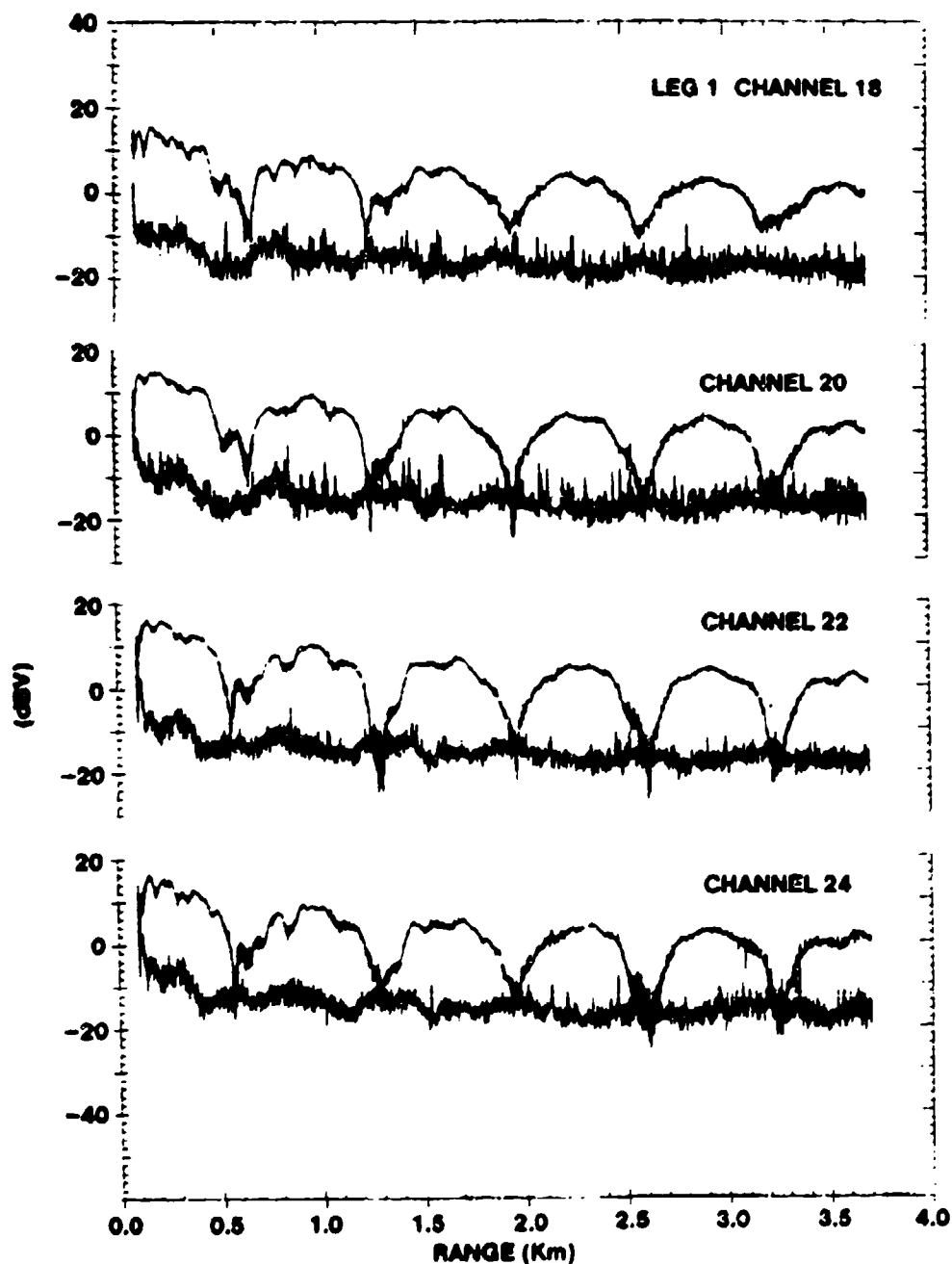
Shown on this viewgraph are two examples of the wavenumber spectra for run TL 2-2. On the left we see the wavenumber spectrum that results from the conventional Fourier-Hankel transform method. Clearly shown are four modal peaks. On the right is the equivalent spectrum obtained without the  $\sqrt{r}$  weighting. This spectra is wholly equivalent to the high resolution Doppler spectra. We observe the values of the horizontal wavenumbers corresponding to each peak remain unchanged, however, the relative modal amplitudes of each mode have changed. For example, the amplitude of mode 2 relative to mode 1 taken from the left hand side is 0.67 compared to 0.82 on the right hand side of the figure. This difference is more pronounced for the third mode, 0.16 to 0.37. The  $\sqrt{r}$  weighting influences those modes which are attenuated most rapidly. It would be possible to measure the change of mode amplitudes as a function of range in this manner, provided the properties of the waveguide do not change or are range independent. The major point made here is that neglecting the  $\sqrt{r}$  weighting does not affect one's ability to determine the modal structure in the waveguide, that is, the propagating wavenumbers.



THE  $\sqrt{r}$  EFFECT: EMPHASIZES THE HIGHER ORDER MODES AS WELL AS CHANGING THE SIDELobe LEVELS AND STRUCTURE.

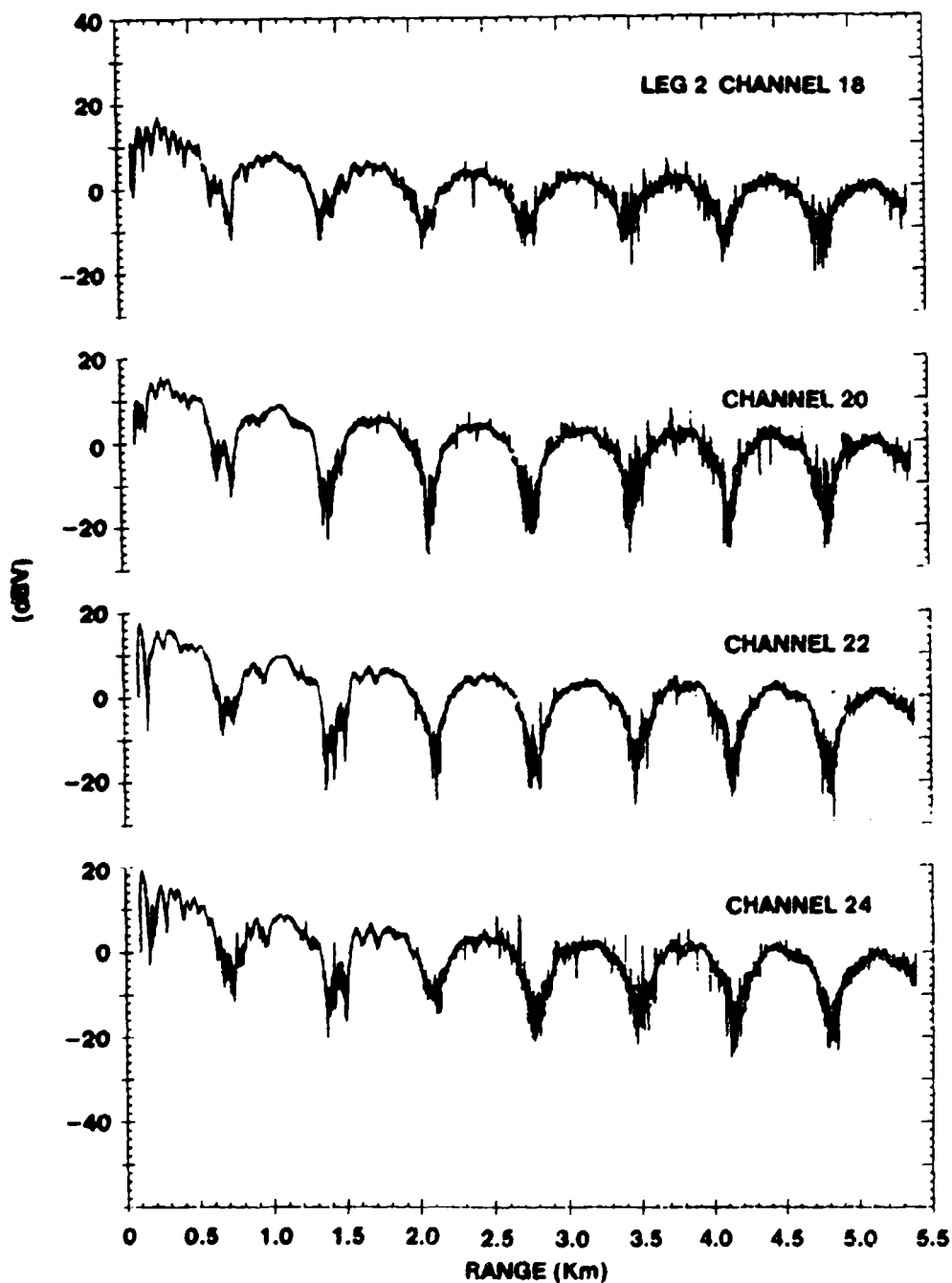
### **Viewgraphs 18, 19 and 20**

These viewgraphs show the relative sound pressure plus noise level as a function of range. These data for TL 2-2 legs 1 (50 Hz), 2 (50 Hz), 3 (75 Hz), show a bimodal structure at the longer ranges with higher order (lower wavenumber) modes superimposed on this underlying structure at shorter ranges. These higher order modes attenuate with increasing range, consistent with the results found in our wavenumber spectra as a result of their mode attenuation values. Thus it would be possible to determine the mode attenuation factors by sequential high resolution wavenumber spectra. This result may be useful in range independent homogenous sedimentary areas. A word of caution is necessary concerning sub-bottom compressional wave profiles and range depth bathymetric effects which could prevent the application of these techniques.



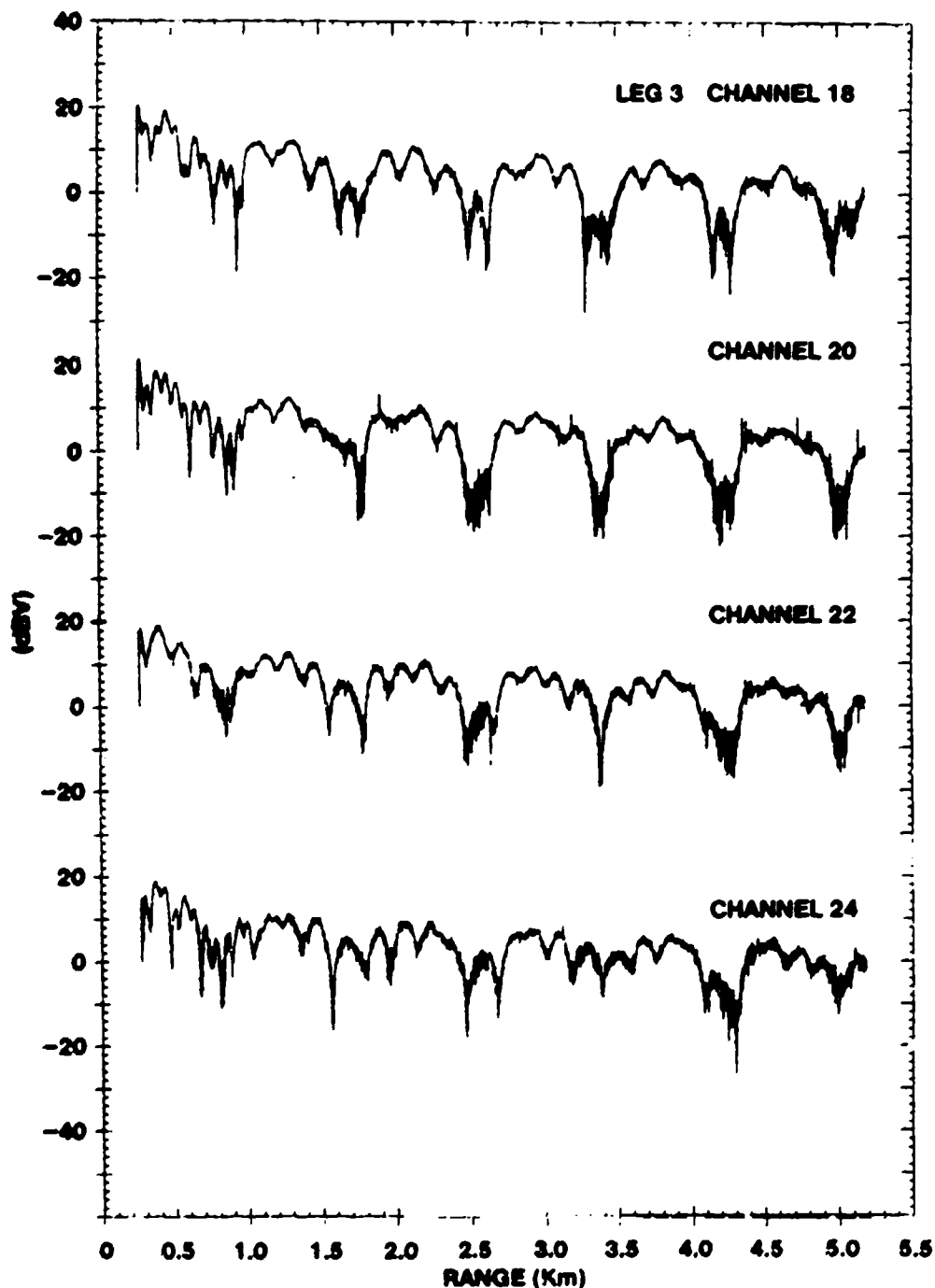
RELATIVE SOUND PRESSURE PLUS NOISE LEVEL VERSUS RANGE: THE DATA ARE SEEN TO HAVE PRIMARILY A BIMODAL STRUCTURE AT LONGER RANGES WITH HIGHER ORDER MODES BEING IMPORTANT AT THE SHORTER RANGES. THE ATTENUATION OF THESE HIGHER ORDER MODES IS CLEARLY ILLUSTRATED IN THE DATA. THUS THE ESTIMATION OF MODAL ATTENUATION MAY BE DONE USING WAVENUMBER SPECTRUM, PROVIDED RESOLUTION CAN BE ACHIEVED.

## VIEWGRAPH 18



RELATIVE SOUND PRESSURE PLUS NOISE LEVEL VERSUS RANGE: THE DATA ARE SEEN TO HAVE PRIMARILY A BIMODAL STRUCTURE AT LONGER RANGES WITH HIGHER ORDER MODES BEING IMPORTANT AT THE SHORTER RANGES. THE ATTENUATION OF THESE HIGHER ORDER MODES IS CLEARLY ILLUSTRATED IN THE DATA. THUS THE ESTIMATION OF MODAL ATTENUATION MAY BE DONE USING WAVENUMBER SPECTRUM, PROVIDED RESOLUTION CAN BE ACHIEVED.

## VIEWGRAPH 19

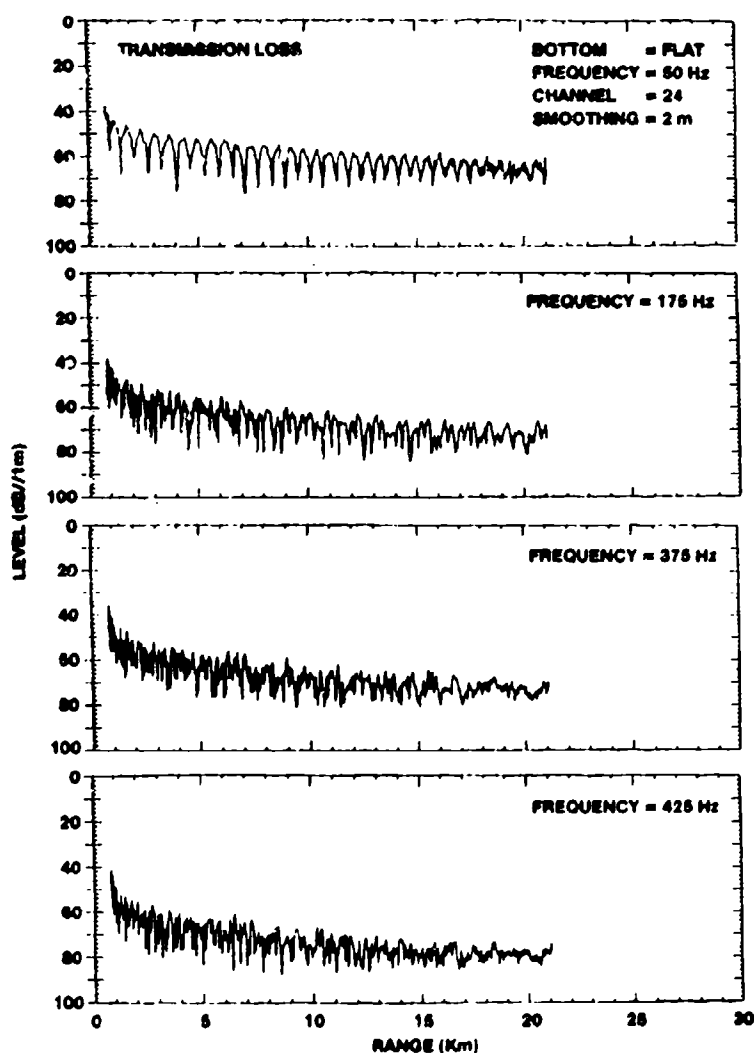


RELATIVE SOUND PRESSURE PLUS NOISE LEVEL VERSUS RANGE: THE DATA ARE SEEN TO HAVE PRIMARILY A BIMODAL STRUCTURE AT LONGER RANGES WITH HIGHER ORDER MODES BEING IMPORTANT AT THE SHORTER RANGES. THE ATTENUATION OF THESE HIGHER ORDER MODES IS CLEARLY ILLUSTRATED IN THE DATA. THUS THE ESTIMATION OF MODAL ATTENUATION MAY BE DONE USING WAVENUMBER SPECTRUM, PROVIDED RESOLUTION CAN BE ACHIEVED.

## VIEWGRAPH 20

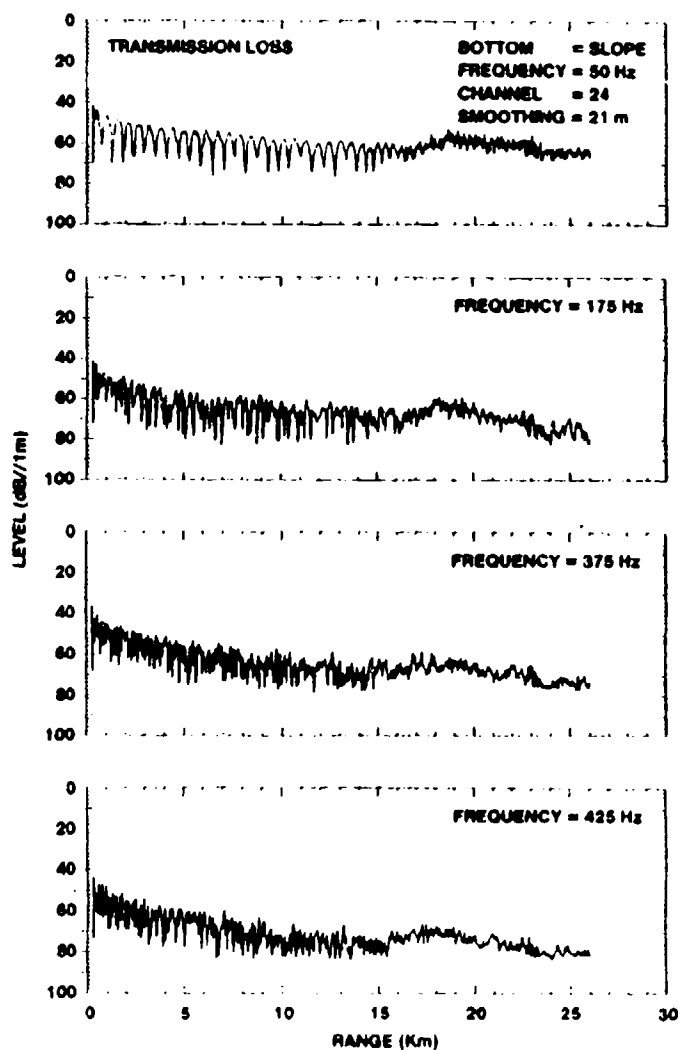
## Viewgraph 21

Longer range runs provided transmission loss data for a flat bathymetry run (viewgraph 21) and a sloping bathymetry run (viewgraph 22). Viewgraph 21 clearly shows the persistence of the bimodal structure at 50 Hz, persisting to a distance on the order of 20 km. One must note that, at this range, our signal-to-noise ratio has decreased to the point that the noise is clearly seen. Given a larger source level, we would expect the structure to remain bimodal. The higher frequencies (175, 375 and 425 Hz) show a very grassy structure at shorter ranges and an evolving pattern at longer ranges. We believe that, at these higher frequencies, a ray description is appropriate. This pattern results from the higher angle rays being absorbed upon repeated bottom interactions, whereas the lower angle rays propagate as up-going and down-coming ray bundles, yielding the more uniform appearance.



## Viewgraph 22

On the other hand, viewgraph 22 shows a slightly different story. One immediately sees a change in the transmission loss at a range of approximately 16 km. This change is caused by the change in bathymetry and the increase in bottom-reflected ship noise. A more subtle change is observed in the 50 Hz data at a distance of 7-9 km. The apparent ship distance changes. The bathymetry is slowly decreasing during this transmission loss run; however, we still see effects in the change in model content at 50 Hz.



## Viewgraph 23

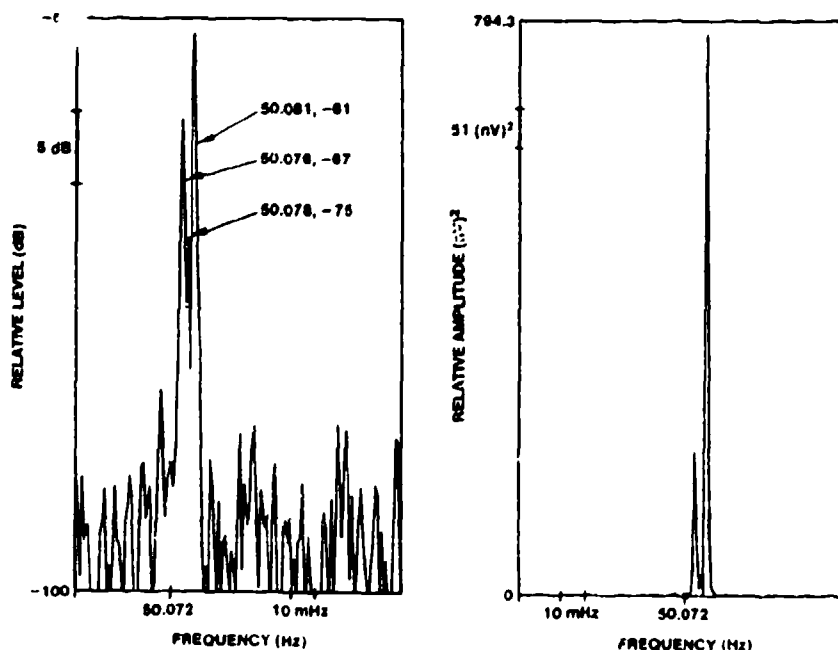
To investigate the range-dependent aspects of the wavenumber spectrum, high resolution Doppler processing was used. Shown on this viewgraph is an HRD spectrum from run TL 3-1, a flat bottom run. On the left is the logarithmic amplitude versus frequency, on the right, the linear amplitude versus frequency. We show both, as the linear plots have been used thus far in our presentation. The linear plot clearly shows two separate modes. The logarithmic plot enables one to see two additional modes, however the logarithmic plot also enhances the noise levels. In the next several viewgraphs I will show logarithmic plots. Shown on the left hand side of this viewgraph are the Doppler-shifted frequencies, each mode, and the relative level in dB re 1 volt. The length of track covered by this spectra is  $\sim 2$  km, and the relative speed is on the order of 2.5 m sec. Under these assumptions, we find that the wavenumber of mode 1 is

$$k_1 = 2\pi \Delta f/v = 0.204,$$

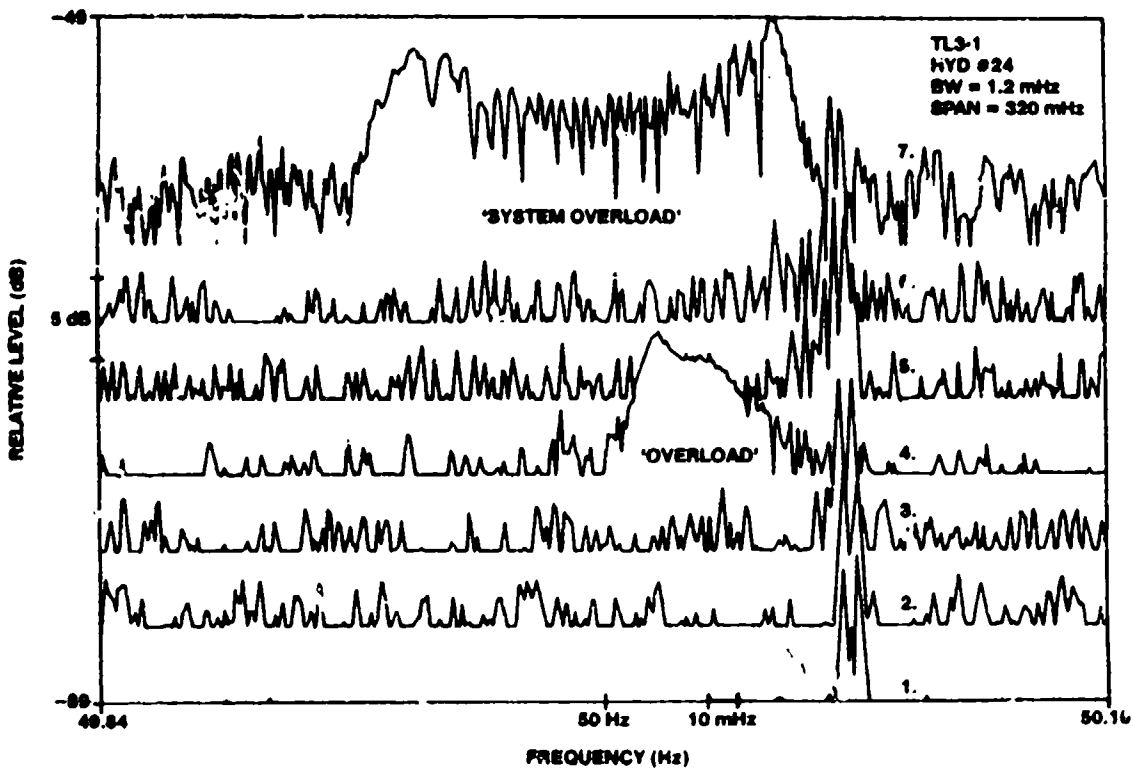
and of mode 2,

$$k_2 = 0.191.$$

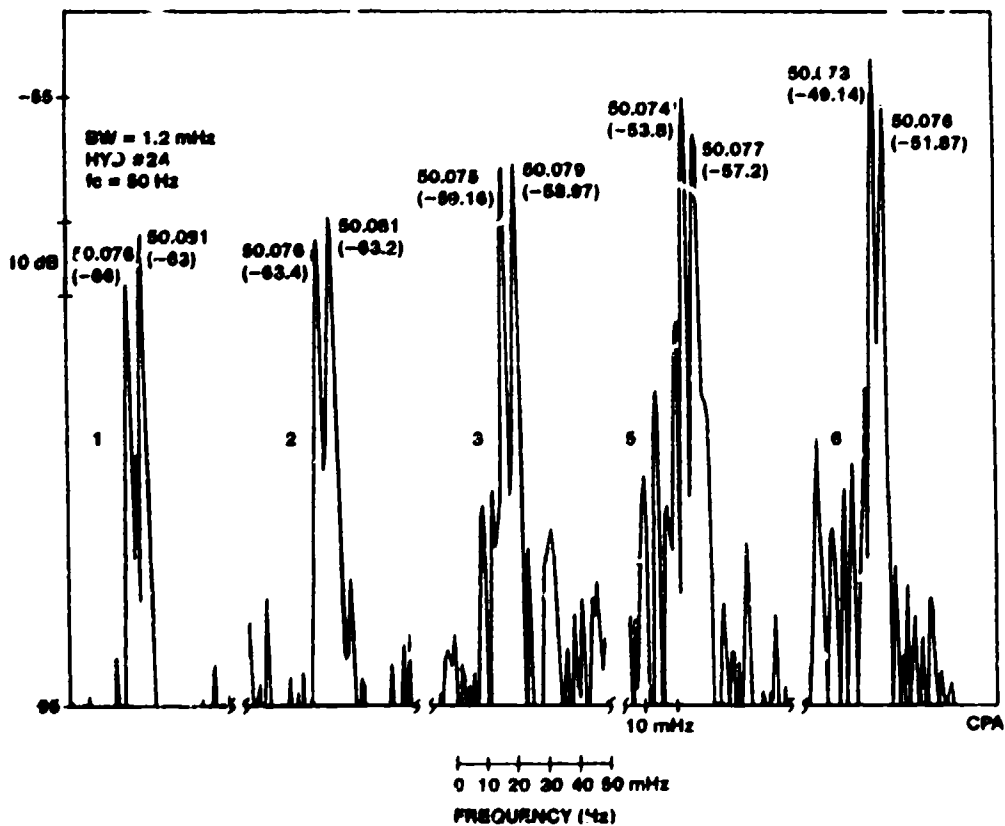
These results compare favorably to the previous values and are remarkable, since the average speed of 5 knots was used.







VIEWGRAPH 24



VIEWGRAPH 25

## Viewgraphs 24 and 25 High Resolution Doppler Processing (TL 3-1, L2, 50 HZ)

These two viewgraphs show the result for the flat bathymetry run. Seven sequential high resolution Doppler spectra are shown for hydrophone 24. Spectra 4 and 7 had a system overload during the measurement interval and were discarded. The resulting spectra are shown on viewgraph 25. Observe the dominant two modes in each spectra. Spectrum number 1 is the range interval most distant from the receiver. Each spectrum covers a range interval of approximately 2 km. The Doppler shifts for each mode and relative level is indicated on the plot.

	MODE 1		MODE 2	
1.	.081	-63 dB	.076	-66 dB
2.	.081	-63.2	.076	-63.4
3.	.079	-58.9	.075	-59.1
4.	--	--	--	--
5.	.077	-57.2	.074	-53.8
6.	.076	-51.8	-.073	-49.1
7.	--	--	--	--

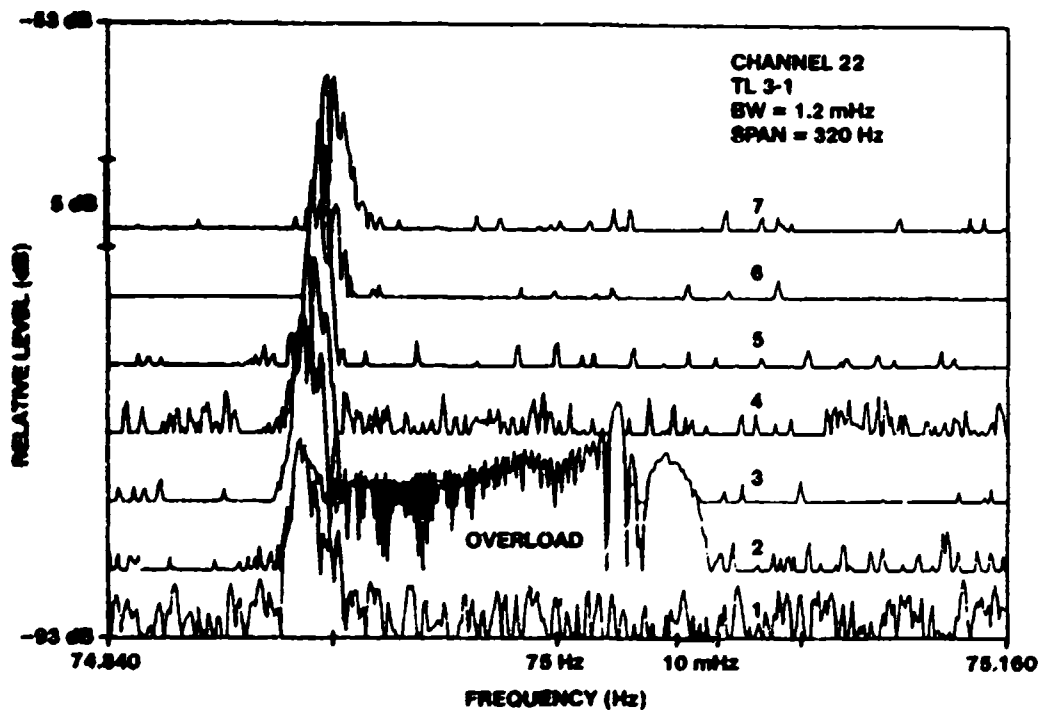
The variations in the Doppler shift are speed related with a means .079 and .075, respectively, corresponding to wavenumbers very close to our theoretical values. The  $\sigma = \pm .002$  clearly brackets our theoretical value.

$$k_1 = 2\pi \Delta f / v = 0.207 \quad \Delta k = \pm .005$$

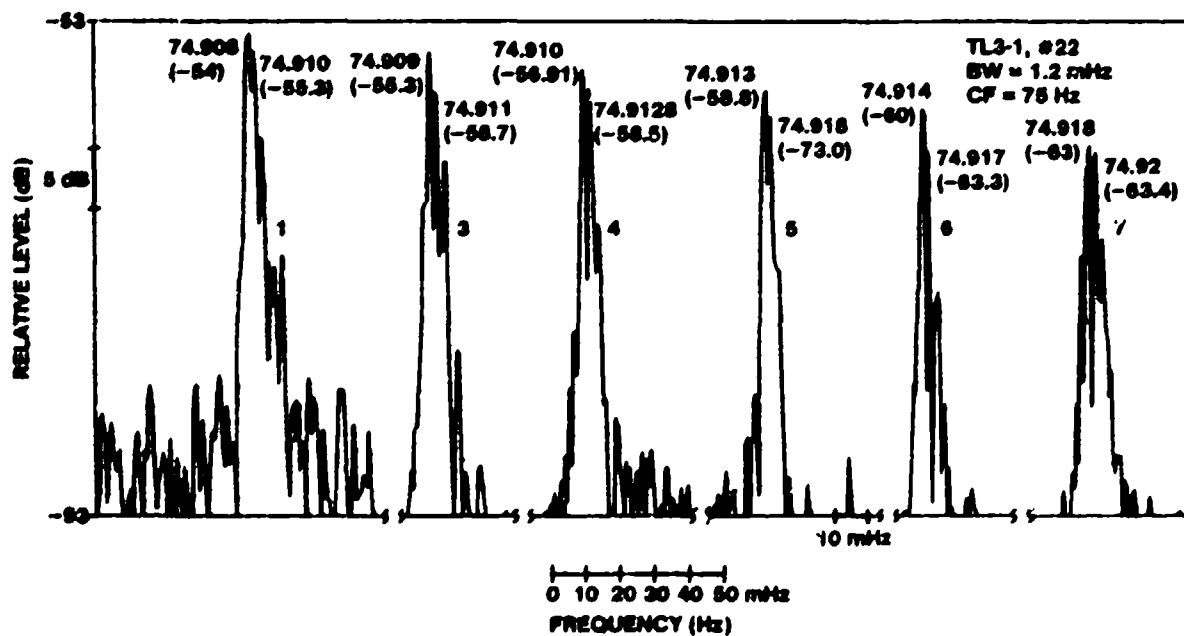
$$k_2 = 0.196 \quad \Delta k = \pm .005$$

These numbers do not reflect changes in ships speed but are based on an av. need of 2.4 msec.

The range variation of each mode is also easily observed. It is clear from the behavior shown on this figure that the higher order modes are attenuated more rapidly than the lowest order mode. This is clearly shown by comparing the behavior of the two dominant peaks with range. Spectrum 6 shows mode 1 to be 2.73 dB higher than mode 2. However, spectrum 1 shows mode 1 to be 3 dB less than mode 2.



VIEWGRAPH 26



VIEWGRAPH 27

### **Viewgraphs 26 and 27 High Resolution Doppler Spectra (TL 3-1, L3, 75 HZ)**

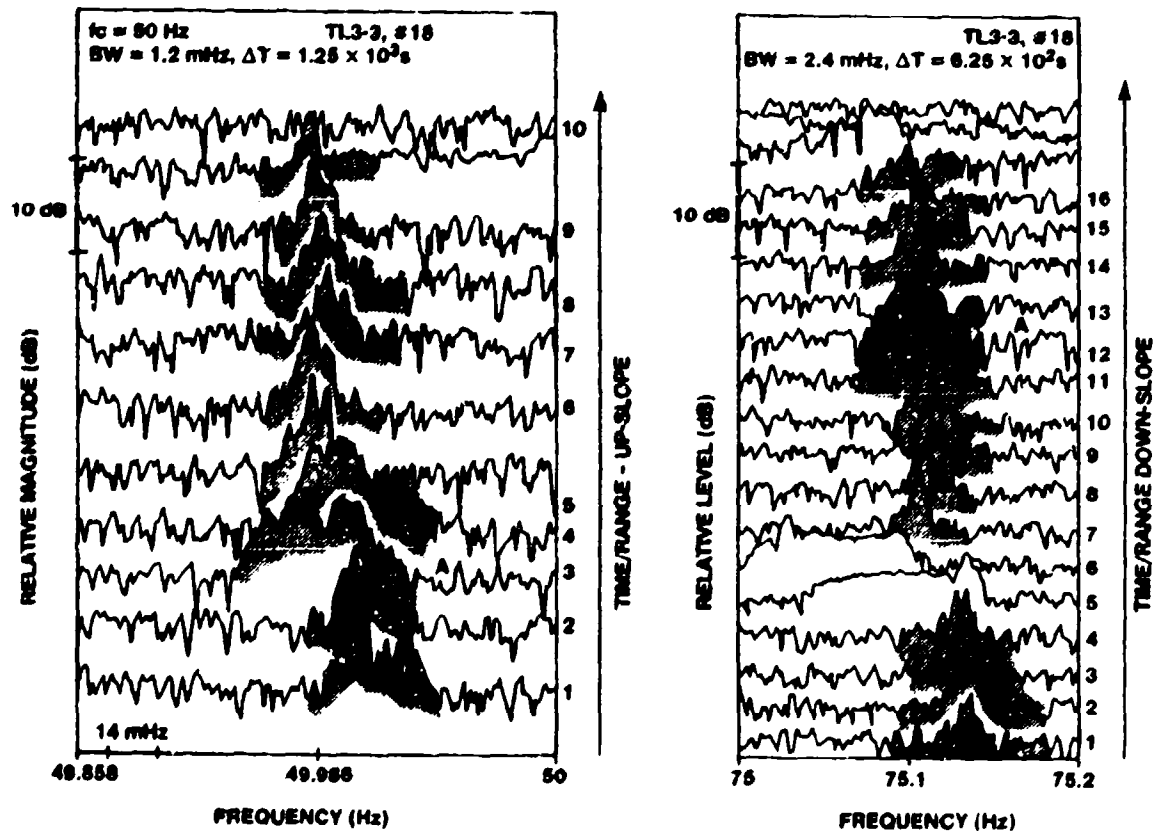
These two viewgraphs show the results at a frequency of 75 Hz. Again the overload spectra were discarded. The six spectra are shown on viewgraph 27. This is an outward bound leg and consequently the Doppler shift is negative. Spectrum 1 is the closest range interval, whereas spectrum 7 is the farthest. The first mode wavenumber from run TL 2-2 was determined to be 0.313, the value determined from these Doppler spectrum using the mean ship's speed yields

$$k_1 = 0.310 \pm .005.$$

The 75 Hz spectrum also yields the attenuation factor for each mode as a function of range. As before, we observe a modal-dependent attenuation factor, the higher order modes attenuated more with distance. With a more accurate real time measurement of relative velocity, these high resolution Doppler spectra yield the horizontal wavenumbers.

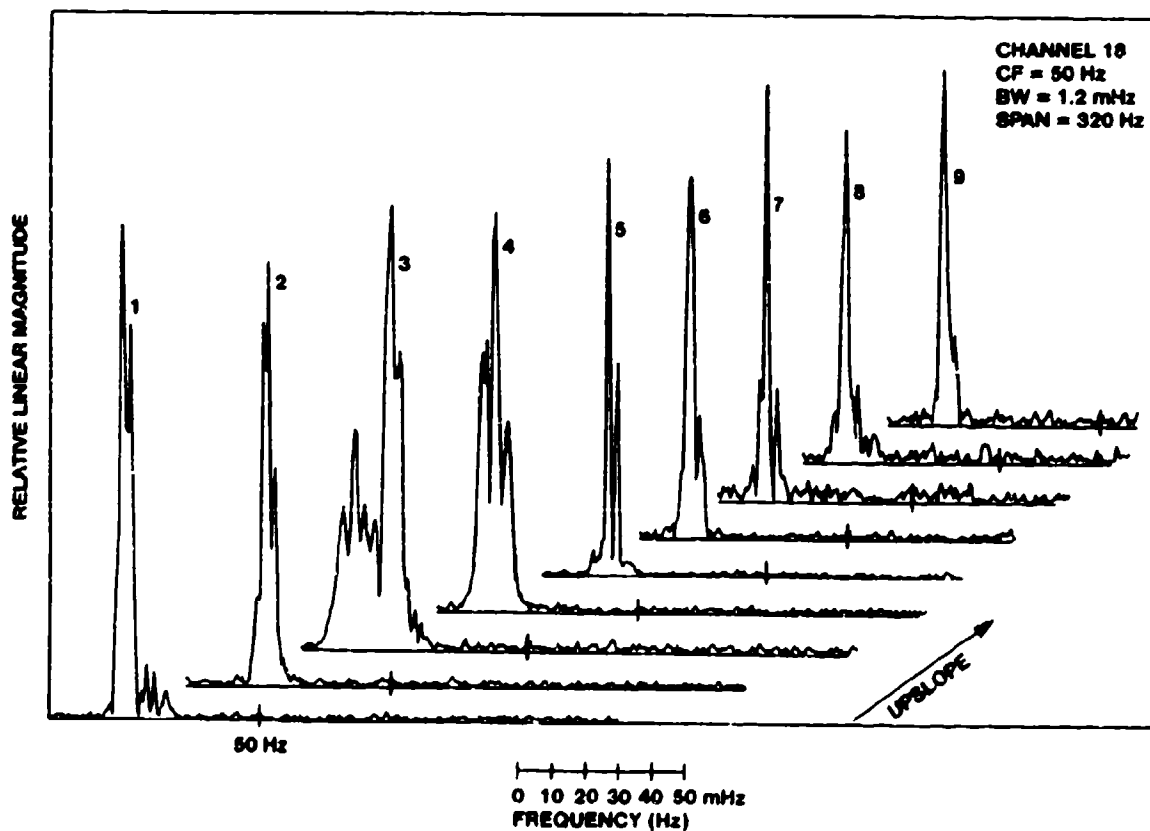
## Viewgraph 28 The Sloping Bottom Case

The flat bathymetry TL runs yielded high resolution Doppler spectra which were similar in structure along the total run. However, the range varying case shown here illustrates a different trend. The left hand side of this viewgraph shows the high resolution Doppler spectrum for the up-slope run at a frequency of 50 Hz; while the right side shows the down-slope run at a frequency of 75 Hz. The unshaded spectra represent system overloading and should be ignored. Spectra number 3 LHS and spectrum number 12 RHS show dramatic change in the modal content not due to speed changes. In general, we observe a range dependence to the wavenumber spectra.



## Viewgraph 29 Linear High Resolution Doppler Spectrum

The 50 Hz, up-slope run is shown here as a series of linear high resolution Doppler spectra. These spectra clearly illustrate the differences between the flat and sloping bottom cases. The variation of modal amplitude with range is variable. The presence (see spectrum number 3) of anomalous features not attributable to speed variations are observed. The particular feature shown in spectra 3 seems to correlate with the variation of the sub-bottom with range. The basic structure revealed in these spectra is range dependent. Whereas the high resolution Doppler spectra yields information concerning the modal structure, it appears to be strongly influenced by the range dependent properties of the waveguide.



## SUMMARY

- CALIBRATED TRANSMISSION MEASUREMENTS SHOWED A REPEATABLE MODAL STRUCTURE
- VARIABILITY OF HORIZONTAL WAVE NUMBERS WERE CONSISTENT WITH
  - WATER COLUMN SVP TEMPORAL AND RANGE VARIATIONS
  - SUBBOTTOM (R&S) FEATURES DEPTH VARIATIONS
- AT LOW FREQUENCIES MODAL WAVENUMBER SPECTRUM CAN BE MEASURED BY
  - FOURIER-HANKEL (FH)OR
  - FOURIER - (HIGH RESOLUTION DOPPLER) METHODS (HRD).  
THE FOURIER-HANKEL TECHNIQUE IS MORE SUITABLE FOR LOW SPEEDS. (<5 KTS) THE HIGH RESOLUTION DOPPLER TECHNIQUE IS MORE SUITABLE AT SPEEDS ~ 5 KTS.
- THESE WAVENUMBERS SPECTRA YIELD MODAL WAVENUMBERS AND ATTENUATION CONSTANTS. INVERSION YIELDS GEOACOUSTIC PROFILES.
- SURVEYS USING EITHER F/H OR HRD COUPLED WITH A TOWED ARRAY AT SPEEDS OF 5 KTS ARE POSSIBLE.

VIEWGRAPH 30

### Viewgraph 30 Summary and Conclusions

An experiment has been performed to measure sound transmission in 73 m of water under calm sea state conditions. The transmission measurements at 50 and 75 Hz showed a repeatable modal interference pattern as a function of range. Calculations performed with SAFARI and measured geoacoustic profiles were found to agree with measurements neglecting shear wave effects. Variations in this pattern were found to be caused by the range dependent bottom and sub bottom features.

The 50 Hz and 75 Hz results were processed using a Fourier-Hankel transform to yield horizontal wavenumber spectra. These horizontal wavenumber spectra were shown to represent biased estimates of the wavenumbers. We were able to eliminate this bias by the constraint  $[k_w^2 = k_h^2 + \beta_v^2]$  and measurements at multiple depths. The variability of the horizontal wavenumber due to processing and water column SVP temporal and range variations is estimated to be  $\pm .005$ . This estimate is consistent with the work of Cederberg.

We showed in this paper that the Fourier-Hankel transform is analogous to high resolution Doppler spectral analysis. This HRD technique was used on the flat bathymetry runs to show the repeatable nature of the horizontal wavenumber spectral characteristic. The advantage of this technique lies in its ease of implementation and ability to be used at higher speeds. The HRD analysis clearly shows the effects of the range-dependent sub-bottom features. On the one hand, these range-dependent effects clearly indicate the change of the effective boundary condition at the sediment sub-bottom interface and illustrate part of the nature of shallow water variability. However these sensitivities to range-dependent characteristics complicate the use of these techniques as survey tools.

In the case of a uniform waveguide these wavenumber spectra yielded modal wavenumber and attenuation constants. Inversions may yield geoacoustic profiles.

It is recognized that surveys using either the FH or HRD techniques and a towed array are possible at survey speeds of 5 kts.



**THIS PAGE INTENTIONALLY LEFT BLANK**

## BIBLIOGRAPHY

- Austin, A., et al., "Huntec 3-D Survey on the Outer Continental Shelf Off New Jersey," Dec. 1990, University of Texas at Austin.
- Carey, W. "Hudson Canyon Experiment" FY88 Ocean Acoustics Report.
- Carey, W., E. Hug, and L. Maiocco, "NUSC-ONR Hudson Canyon Experiment," NUSC FY88 IR Report, TR 8487, 2-3 to 2-7, April 7, 1989.
- Carey, W., and L. Maiocco "NUSC/ONR Hudson Canyon Experiment," NUSC FY89 IR Report, TR 8707, April 6, 1990.
- Carey, W., and J. Bishop, "Shallow Water Wavenumber Spectrum Measurement," Submitted as an FY 90 Significant R and D Accomplishment".
- Carey, W., and L. Maiocco Dillman, "NUSC/ONR Hudson Canyon Experiment," NUSC FY 90 IR/IED Report, TR 8871, 2-5 to 2-8, April 1991.
- Carey, W., J. Doult, and L. Maiocco Dillman, "Shallow-Water Transmission Measurements Taken on the New Jersey Continental Shelf," 121st Meeting, Acoustical Society of America, 2 May 1991.
- Cederberg, R. J., W. L. Siegmann, M. J. Jacobson, and W. Carey, "Predictability of Acoustic Intensity in Shallow Water at Low Frequencies Using the Parabolic Approximation," Paper 3UW11, 121st Meeting, Acoustical Society of America, 30 April 1991.
- Cederberg, R.J., W L. Siegmann, M. J. Jacobson, and W. Carey, "Predictability of Acoustic Intensity in Shallow Water at Low Frequencies Using Parabolic Approximation," Paper 3UW11, Journal of the Acoustical Society of America, vol. 89, No.4, Pt.2, April 1991.
- Frisk, G. V. and J. F. Lynch, "Shallow Water Wave Guide Characterization Using the Hankel Transform," Journal of the Acoustical Society of America, vol. 76, no. 1, July 1984, pp. 205-216.
- Frisk, G.V., J. F. Lynch, and J. A. Doult, "The Determination of Geoacoustic Modal in Shallow Water," in Ocean Seismo-Acoustics, etc. T. Akal and J. Berkson, 693-702, Plenum Press, N.Y. 1985
- Lynch, J. F., S. D. Rajan, and G. Frisk, "A Comparison of Broadband and Narrowband Modal Inversions for Bottom Geoacoustic Properties at a Site Near Corpus Christi, Texas," Journal of the Acoustical Society of America, vol. 89, no. 2, 1991, pp. 648-665.
- Maiocco, L., W. Carey, E. Parssinen, and J. Doult, "Measurement of Shallow Water Sound Transmission on the New Jersey Continental Shelf" paper C9, 118th Meeting, Acoustical Society of America, Journal of the Acoustical Society of America, vol. 86 (s1), Fall 1989.
- Maiocco, L. "An Experimental Investigation of an Acoustic Technique to Determine Shallow Water Bottom Boundary Impedance," University of Connecticut, June 1990.(Also as NUSC TR 8839, June 1991).

- Rogers, A. K. and T. Yamamoto, "Measurement and Modeling of Acoustic Waves in the 50- to 600-Hz range at the Hudson Canyon Site," Paper 5UW6, 120th Meeting, Acoustical Society of America, Journal of the Acoustical Society of America, vol. 88 (SI), Fall 1990.
- Rogers, A. K., T. Yamamoto, F. Tappert, and W. Carey, "Remote Sensing of Seabed Compressions Wave Attenuation From Acoustic CW Propagation Experiments Combined with the Bottom Shear Modales Profiler (BSMP) Database," Paper 30C4, Journal of the Acoustical Society of America, vol. 89 (4,pt. 2), April 1991.
- Werbey, M. F. and G. J. Tango, "Characterization of Average Geoacoustic Bottom Properties From Expected Propagation Behavior at Very Low Frequencies (VLF) Using a Towed Array Simulation," in Ocean Seismo-Acoustics, etc. T. Akal and J. Berkson, Plenum Press, New York, 1985, pp. 881-889.

# INITIAL DISTRIBUTION LIST

Addressee	No. of Copies
CNA	3
DTIC	2
DARPA UWO (Dr. William Carey)	2
DARPA (C. Stuart)	5
CNO (OP-952; NOP-096)	2
CNR (OCNR-00, -10; -11; -1125 Marshall Orr, L. Johnson, R. Roracta, A. Brandt; -13 K. Dial, M. Briscoe; E. Chaika; ONT -23)	11
NAVAIRSYSCOM (NAIR-93; -933)	2
SPACE & NAV WARFARE SYS CMD (PMW-180 J.P. Feuillet, J. Synsky, CAPT K. Evans, CAPT R. Witter)	4
NAVSEASYSOM (SEA-63)	1
NRL (NRL 5100 B. Bradley; 5120, 5160, F. Erskine, W. Kuperman, B.E. McDonald; 5130 N. Yen, TD W. Moseley, 200 R. Wagstaff, E. Franchi; 24C R. Farvell, H. Assanai)	11
NADC	1
NCSC (D. Fields)	1
NOSC (541B H. Bucker (3 cys)	3
DTIC CADEROCK LAB (M. Strassberg; M. Sevic (3 cys)	4
NPS	2
APL/JOHN HOPKINS (G. Smith (3 cys)	3
JOHN HOPKINS UNIVERSITY (Mechanical Enginee Dept) (A. Prosperetti (3 cys), E. Fitzgerald)	4
APL/U WASHINGTON (R. Spindel (2 cys),	2
APL/PENN STATE (S. McDaniels (2 cys), D. McGammaon, R. Goodman)	4
APL/U TEXAS (K. Focke, J. Shooter, P. Vidmar, E. Westwood, S. Mitchell, N. Bedford)	6
NPL/SCRIPPS (F. Fisher, W. Hodgkiss, M. Buckingham, D. Jacobs, S. Webb)	5
WOODS HOLE OCEAN INSTI. (S. Rajan, G. Frisk, J. Lynch, J. Douth)	4
U. OF MIAMI (F. Tappert, H. DeFarrari, T. Yamamoto)	3
U. OF MISS. (L.A. Crum, R.A. Roy, S.W. Yoon, A.R. Kolaini, M. Nicholas)	3
SAI CORP., McLean, VA (A. Eller, R. Cavanaugh, C. Spofford)	3
SAI CORP., New London, CT (F. DiNapoli, R. Evans, W. VonWinkle)	3
PSI, McLean, VA (J. Barberra)	2
PSI, Sledell, LA (M. Bradley)	2
PSI, New London, CT (J. Davis)	2
TRW (S. Gerben)	1
MIT OCEAN ENGINEERING DEPARTMENT (I. Dyer, K. Meville, A. Baggeraer, H. Smedt)	4
U. CONN. AVERY POINT, (E. Monahn, Dr. R. Mellen)	2
RPI, TROY, NEW YORK 12180, DEPT OF MATH (W. Siegmans, R. Cederberg)	4
GEORGIA TECH. (P. Rogers)	2
CATHOLIC UNIVERSITY (J. McCoy)	3
BBN, Arlington, VA (H. Cox, J. Mitsche)	2
BBN, New London, CT (P. Cable, W. Marshall, J. Hanrahan, S. Marshall)	4
BBN, Cambridge, MA (J. Barger, R. Collier, J. Heines)	3